

1-1-2011

First steps in assessing microbial involvement in the geochemical evolution of uranium mine tailings : evaluation of iron reduction potential, biofilm formation and community heterogeneity

Virgil C. Guran
Ryerson University

Follow this and additional works at: <http://digitalcommons.ryerson.ca/dissertations>

 Part of the [Biology Commons](#)

Recommended Citation

Guran, Virgil C., "First steps in assessing microbial involvement in the geochemical evolution of uranium mine tailings : evaluation of iron reduction potential, biofilm formation and community heterogeneity" (2011). *Theses and dissertations*. Paper 704.

This Thesis is brought to you for free and open access by Digital Commons @ Ryerson. It has been accepted for inclusion in Theses and dissertations by an authorized administrator of Digital Commons @ Ryerson. For more information, please contact bcameron@ryerson.ca.

FIRST STEPS IN ASSESSING MICROBIAL INVOLVEMENT
IN THE GEOCHEMICAL EVOLUTION OF URANIUM MINE
TAILINGS: EVALUATION OF IRON REDUCTION
POTENTIAL, BIOFILM FORMATION AND COMMUNITY
HETEROGENEITY

By

Virgil C Guran, BSc. Applied Chemistry and Biology
Ryerson University, Toronto, Canada, 2008

A thesis
presented to Ryerson University
in partial fulfillment of the
requirements for the degree of
Master of Applied Science
in the Program of
Environmental Applied Science and Management

Toronto, Ontario, Canada 2011

©Virgil C Guran 2011

I hereby declare that I am the sole author of this thesis.

I authorize Ryerson University to lend this thesis to other institutions or individuals for the purpose of scholarly research.

I further authorize Ryerson University to reproduce this thesis by photocopying or by other means, in total or in part, at the request of other institutions or individuals for the purpose of scholarly research.

FIRST STEPS IN ASSESSING MICROBIAL INVOLVEMENT IN THE GEOCHEMICAL EVOLUTION OF URANIUM MINE TAILINGS: EVALUATION OF IRON REDUCTION POTENTIAL, BIOFILM FORMATION AND COMMUNITY HETEROGENEITY

Master of Applied Science, 2011

Virgil C Guran

Environmental Applied Science and Management, Ryerson University

ABSTRACT

The high pH (~10) and elevated concentration of metals and oxyanions such as As, Fe, Ni, Mo and Se in the Deilmann tailings management facility (DTMF) presents a highly selective environment for microorganisms. The objective of this study was to assess the potential for metal and ion solubilization by the indigenous mixed microbial community in both optimum (high carbon) and *in-situ* (low carbon alkaline environment) conditions in terms of bulk pH and redox potential in order to satisfy the requirement for calculating long term stability. A flow-cell system was developed in order to monitor the extent of microbial metal reduction as well as determine biofilm formation by tailings-isolated mixed communities. The microbial consortium isolated from the DTMF has shown the ability to reduce ferric iron for energy conservation under both carbon conditions.

AKNOWLEDGEMENTS

I would like to express my gratitude to the following:

My thesis supervisor, Dr. Gideon Wolfaardt for his support and guidance, without who's trust I would not be where I am today professionally;

The members of my thesis examining committee, Dr. Martina Hausner, Dr. Kimberley Gilbride and Dr. Michal Bardecki for their valuable comments and helpful criticism;

The members of Dr. Gideon Wolfaardt's research laboratory for their assistance and guidance throughout my research;

Dr. Darren Korber and his research team for their wonderful collaboration and help that have made my research much more delightful;

Dr. Tom Kotzer (CAMECO Corp.) for his valuable insight and support;

Battista Calvieri for the help and valuable training experience with scanning electron microscopy imaging at the University of Toronto;

Ryerson University and CAMECO Corp. for financial support and opportunity to visit Key Lake, northern Saskatchewan;

My parents for their unconditional love and support as well as my friends for their continuous understanding;

My fiancée, Catalina, for her indispensable support and encouragement; her constant involvement was crucial to the successful completion of this work.

TABLE OF CONTENTS

ABSTRACT.....	iii
ACKNOWLEDGEMENTS	iv
TABLE OF CONTENTS.....	v
LIST OF TABLES.....	vii
LIST OF FIGURES.....	ix
INTRODUCTION.....	1
CHAPTER 1: LITERATURE REVIEW	4
1.1 Tailings Management Facilities: Solutions for Uranium Production Waste Disposal	4
1.2 Implications of Heavy Metal Chemistry.....	6
1.2.1 Iron in Anaerobic Environments: Valuable Microbial Energy Source.....	6
1.2.2 Iron speciation and availability: A Function of Redox Potential and pH	7
1.3 Arsenic: Co-precipitation and sorption to heavy metal complexes	10
1.4. Microbiology of Metal Reduction	12
1.4.1 The Benefits of the Biofilm Matrix.....	12
1.4.2 Microbial Iron Reduction in the Environment.....	13
1.4.3 Diversity among Iron Reducers.....	15
1.4.4 Redox Metabolic Activities	17
CHAPTER 2: METHODOLOGY	25
2.1 Site location and site description.....	25
2.1 Core Sampling	26
2.2 Bacterial Culturing	27
2.3 The Flow-cell system.....	28
2.3.1 Flow-cell Inoculation	33
2.4 Analytical Analysis.....	33
2.4.1 The FerroZine Method	33
2.4.2 OR probe preparation and data recording	35

2.5 Microscopy	36
2.5.1 Confocal Laser Scanning Microscopy (CLSM)	36
2.5.2 Scanning Electron Microscopy (SEM)	36
2.6 Molecular Analysis	38
2.6.1 Genomic DNA extraction	38
2.6.2 PCR amplification of 16S rRNA genes for produced water and seawater DGGE ..	38
2.6.3 Microsom bacterial community Denaturing Gradient Gel Electrophoresis (DGGE) analysis.....	39
CHAPTER 3: RESULTS AND DISCUSSION.....	40
3.1 Aerobic and anaerobic enrichments.....	40
3.2 Redox Potential Measurements of Continuous Flow-Cell Systems.....	42
3.3 Ferrous Iron Production in Continuous Flow-Cell Systems	46
3.4 Microscopy of Attachment Substrate: Confocal Laser Scanning and Scanning Electron Microscopy.....	50
3.5 Molecular Work and Identification of Mixed Community Members	60
CHAPTER 4: CONCLUSIONS	63
4.1. Concluding Statement.....	63
4.2 Future Directions: Opportunities for Microbiological Studies	64
REFERENCES	66
APPENDICES	72
<i>Appendix 1: Physical and Chemical Measurements of DTMF Core Samples</i>	<i>72</i>
<i>Appendix 2: Redox Potential Measurements: Continuous recorded OR values.</i>	<i>73</i>
<i>Appendix 3: Ferrous Iron Concentration Measurements - The Ferrozine Method.</i>	<i>75</i>

LIST OF TABLES

Table 1.1. Scale of Redox Potentials and oxidation potentials measured with a platinum electrode. For the soil conditions given, the measurement is <i>in situ</i> (Adaptation from Jackson 2005).....	8
Table 2.1. LB Aerobic Medium used for enrichment purposes.....	27
Table 2.2. Anaerobic Ferric Lactate Medium used for flow system and enrichment purposes.	28
Table 2.3. Ferric Lactate medium used for nutrient poor flow-cell experiments.	31
Table 2.4. Preparation of Ferrous iron standards for the FerroZine colorimetric method....	34
Table 2.5. Relationship between Relative Eh and Absolute Eh required for ORP calibration.	35
Table 2.6. Description of procedure for CLS imaging.	36
Table 3.1. DGGE band sequencing results.	62
Table A1.1 Physical and chemical measurements of the DTMF cores at the E2 site.	72
Table A2.1 Raw OR data sample recorded with the Symphony® SP70P portable pH/OR meter, in a mixed community flow-cell under low-carbon conditions at pH 9.5.	73
Table A2.2 Redox Potential Measurements of flow-cells under high carbon conditions at pH 7.0.	74
Table A2.3 Redox Potential Measurements of flow-cells under low carbon conditions at pH 9.5.	74
Table A3.1 Fe(II) standards for Mixed Community flow-cell, high carbon, neutral pH.....	75
Table A3.2 Mixed Community flow-cell samples ferrozine absorbance values.	76
Table A3.3 Mixed Community Fe(II) concentrations in high carbon neutral pH flow-cell.	76
Table A3.4 Positive Control Fe(II) concentrations in high carbon neutral pH flow-cell.	77

Table A3.5 Sterile Control Fe(II) concentrations in high carbon neutral pH flow-cell..... 77

Table A3.6 Mixed Community Fe(II) concentrations in low carbon flow-cell, pH 9.5..... 78

Table A3.7 Positive Control Fe(II) concentrations in low carbon flow-cell, pH 9.5. 78

LIST OF FIGURES

Figure 1.1. Representation of the Athabasca Basin, northern region of Saskatchewan rich in high grade uranium ore, showing the locations of the two largest uranium mills in the world (Key Lake and Rabbit Lake) and world's largest high-grade uranium mines (McArthur River and Cigar Lake) (adopted from Cameco Corp. 2010).	4
Figure 1.2. Cross-sectional area of the DTMF, showing depth variation and previous sampling points (adopted from Maathuis 2010).	5
Figure 1.3. Stability field diagram for dissolved and solid forms of iron as a function of pH and Eh at 1atm and 25°C (adopted from Elder 1988)	9
Figure 1.4. Mechanisms of iron reduction via direct (A) and Indirect (B) (mediated) methods (adopted from Lloyd 2003).	18
Figure 1.5. Transmission electron micrograph showing the distribution of c-type cytochromes in the outer membrane in <i>S. oneidensis</i> (A) and <i>Pelobacter carbinolicus</i> cell lacking such cytochromes (adopted from Lloyd 2003).	20
Figure 2.1. Locations of the 1999, 2004/2005, 2008 and 2009 boreholes and monitor wells; the large red marker represents the location of this study's sample location (E2 borehole).	25
Figure 2.2. Design of the Flow-cell housing and chamber, constructed from an 8.0cm x 5.5cm x 1.5cm block of plexiglass.	29
Figure 2.3. Representation of a packed sterile flow-cell (A) and a flow-cell connected to the flow system (B), packed with attachment substrate.	30
Figure 2.4. Schematic of the anaerobic continuous flow system created to study microbial metabolic activity, showing the major components.	30
Figure 2.5. Illustration of the modified rubber stoppers used to seal the synthetic feed and maintain it sterile and anaerobic; only the headspace pressure and flow-cell ports were closed during autoclaving; only the headspace pressure port was closed during N ₂ purging; only autoclaving pressure release port was closed while running the flow system.	32
Figure 3.1. Anaerobic serum vials showing (A) color of sterile Fe(III) enrichment medium, (B) color change of Fe(III) medium inoculated with <i>S. putrefaciens</i> as a positive control, color	

change and precipitate of Fe(III) pH 7.5 medium (C) and pH 9.5 medium (D) inoculated with tailings material.	40
Figure 3.2. Visual determination of Fe(III) reduction and color change of synthetic feed of <i>S. putrefaciens</i> , sterile control and mixed community flow-cells after 1 day of incubation (A1, A2, A3) and after 3 days of incubation (B1, B2, B3).....	41
Figure 3.3. Graphical representation of the change in Eh in flow-cell systems over an 8 day incubation period under high carbon (0.9g/L) neutral pH conditions.	43
Figure 3.4. Graphical representation of the change in Eh in flow-cell systems over an 8 day incubation period under low carbon (20mg/L lactate and citrate), alkaline conditions.....	45
Figure 3.5. Ferrous iron concentrations recorded in flow-cell systems under high carbon conditions at neutral pH.	47
Figure 3.6. Ferrous iron concentrations recorded in flow-cell systems under low carbon conditions at alkaline pH.	48
Figure 3.7. A closer look at the relationship between Fe(II) concentration values in a mixed community flow-cell over the duration of low carbon incubation.	49
Figure 3.8. An <i>in-situ</i> CLSM image (60X-oil immersion) of a high carbon flow-cell chamber showing considerable amounts of biomass at the clay-liquid interface, after an 8-day incubation period suggesting biofilm formation.	51
Figure 3.9. An <i>in-situ</i> epifluorescence microscopy image (60X–oil immersion) of a high carbon flow-cell chamber showing EPS production by microbial cells and colonization of the clay-sand substrate, at neutral pH.....	52
Figure 3.10. SEM image of biofilm formation by the mixed community on the surface of the attachment substrate under high carbon conditions at neutral pH.	53
Figure 3.11. SEM image showing EPS connecting strands in the biofilm network under high carbon conditions at neutral pH.	54
Figure 3.12. SEM image showing relationship between bacterial cells and the EPS strand network under high carbon conditions at neutral pH.	55
Figure 3.13. SEM image showing close interaction between microbial cells and production of EPS connecting network in a micro-environment on the attachment substrate, under high carbon neutral pH conditions.	56

Figure 3.14. Epifluorescence microscopy image (60X-oil immersion) of a low carbon flow-cell chamber showing limited microbial growth on the attachment substrate and significant decrease in microbial cellular size, pH 9.5..... 57

Figure 3.15. Epifluorescence microscopy image (60X-oil immersion) of a low carbon flow-cell chamber showing random growth of bacterial cells in small aggregates, pH 9.5..... 58

Figure 3.16. SEM image showing a single bacterial cell rather than biofilm formation on attachment substrate material, an effect of carbon deprivation..... 59

Figure 3.17. SEM image showing absence of biofilm formation and channeling created by preferential flow of synthetic feed on attachment substrate under low carbon conditions, at pH 9.5..... 59

Figure 3.18. DGGE image showing 4 distinct bands for enrichment sample #60 used in this study, against other samples enriched under similar conditions..... 60

Figure A3.1. Fe(II) Standard Curve, Mixed community samples, high carbon, neutral pH. ... 75

INTRODUCTION

Thesis Synopsis

In a constant effort to meet the demand for energy, Canada plays an important role world-wide, as the largest provider of high grade uranium for nuclear power plants, accounting for roughly one third of the global output (Natural Resources Canada 2009). Economically, the mining and milling of uranium in Canada is a \$500 million a year industry, providing numerous employment opportunities across the country (Natural Resources Canada 2009). It has been claimed that nuclear power is the most environmentally friendly method of producing electricity on a large scale. Currently, nuclear energy growth rate is faster than liquid fuels, natural gas and coal in all end-use sectors except transportation, and it provides 14% of the world's electricity (World Nuclear Association 2010; U.S. Department of Energy 2010). With the projected growing demand for electrical energy by 2.3% per year between 2007 and 2035, it is imperative that the impact of nuclear waste production from uranium mining and milling be determined on a long term scale (U.S. Department of Energy 2010). Uranium mine and mill tailings are low-level radioactive wastes produced in Canada (Natural Resources Canada 2009). Presently, tailings are deposited in large in-pit facilities covered with water to reduce the release of gamma radiation and radon gas (Natural Resources Canada 2009). The tailings material consolidates and settles in an impermeable body, with a low hydraulic conductivity between itself and the groundwater thus minimizing the possible interaction between the two (Wolfaardt *et al.*, 2008; Natural Resources Canada 2009).

At the Deilmann tailings management facility (DTMF), Key Lake, Saskatchewan, the tailings material contain high concentrations of Ni (2%) and As (1.2%), metals generally associated with other insoluble complexes such as ferrihydrite and ferric (hydr)oxides (Tessier *et al.*, 1996). There have been numerous studies which explained heavy metal behaviour in mine tailings from a geochemical and geotechnical perspective (Hudson-Edwards *et al.*, 1999; Donahue *et al.*, 2003; Moldovan *et al.*, 2008); however, relatively few

studies have focused on microbial activity in such oligotrophic extreme environments such as the DTMF sediment: alkaline pH (9-10), low temperatures (4-5°C) and low total organic carbon (10-20mg/L) (Maathuis 2010). Microbial activity can play an important role in the transport of radionuclides and other heavy metals in the environment (Panak *et al.*, 1998). Through direct and indirect metal reduction metabolic pathways either for energy conservation or other metabolic requirements, specialized groups of microorganisms can potentially alter the geochemical aspect of uranium mine tailings on a long term scale by solubilization of heavy metals (Lloyd 2003, Wolfaardt *et al.*, 2008).

Most studies that have investigated microbial metal reduction have been focused on pure cultures of dissimilatory iron reducing bacteria (DIR), which are known to reduce various forms of ferric iron (Fe(III)) and cause solubilization of associated heavy metals (Coates *et al.*, 1996, Cummings *et al.*, 1999, Kostka *et al.*, 2002). In contrast, the objective of this research was to determine microbial metabolic activity of mixed communities isolated from the DTMF sediment in terms of ferric iron reduction and biofilm formation under favorable growth conditions, as well as oligotrophic high pH, low organic carbon conditions, in an anaerobic environment. To achieve this, a conventional continuous flow-cell system (Bester *et al.*, 2005) was modified to allow for simultaneous real-time monitoring of metabolic activity (redox potential) as well as biofilm formation (confocal laser scanning and scanning electron microscopy). Microbial Fe(III) reduction was determined by measuring concentrations of Fe(II) produced in the flow-cell at fixed time intervals. Bacterial cells were provided with an attachment substrate composed of kaolinite clay and sand, on which biofilms could develop. The synthetic feed passed through the system with the use of a peristaltic pump at a rate of 1.43m/hr at the clay/liquid interface, contained two carbon sources (lactate and acetate) chosen for their known use by microorganisms capable of Fe(III) reduction (Coates *et al.*, 1996, Kostka *et al.*, 2002), as well as the source of Fe(III) in soluble form. The synthetic feed was also amended with yeast extract to supply the necessary vitamins required for bacterial growth. The nutrient content between the two sets of experiments was changed to determine microbial growth under oligotrophic conditions; however, Fe(III) concentrations were maintained constant for pattern recognition. The positive control was the iron reducer *Shewanella putrefaciens* in pure culture (ATCC BAA-

1097™). As a final step, the mixed community was sequenced in order to determine the identity of the dominant bacterial species, using basic techniques of molecular biology.

Hypothesis

It was hypothesized that the redox potential in the sediment of the DTMF is influenced by facultative anaerobic microbial activity acting as a biocatalyst on the reduction of insoluble metal complexes such as ferrihydrite or ferric (hydr)oxide thus causing solubilization of associated heavy metals. Although reductive dissolution of ferric iron is possible at a micro-scale level, the impact on the bulk tailings body is not known.

Objectives

The main objectives of this study were to determine (i) the rate of microbial Fe(III) reduction, and (ii) formation potential of biofilm by the tailings-isolated mixed community under both favorable and *in-situ* conditions in terms of carbon content and pH; and to compare these rates with the positive control *S. putrefaciens*. This was achieved by creating a flow-cell system which measured, in real time, microbial activity through redox potential (Eh), allowed specific time interval sampling for Fe(II) concentrations determination, and facilitated confocal laser scanning and scanning electron microscopy imaging for biofilm architecture investigation.

CHAPTER 1: LITERATURE REVIEW

1.1 Tailings Management Facilities: Solutions for Uranium Production Waste Disposal

Canada's Athabasca Basin holds the world's largest high grade uranium mill at Key Lake, Saskatchewan (Figure 1.1), with an annual licensed milling capacity of 8.5 million kilograms of U_3O_8 (Cameco Corp. 2010).



Figure 1.1. Representation of the Athabasca Basin, northern region of Saskatchewan rich in high grade uranium ore, showing the locations of the two largest uranium mills in the world (Key Lake and Rabbit Lake) and the world's largest high-grade uranium mines (McArthur River and Cigar Lake) (adopted from Cameco Corp. 2010).

Due to the high purity of the uranium ore found in the mines of northern Saskatchewan (McArthur River mine ore being up to 100 times the world's average), the slurry transported to Key Lake Mill for processing must be blended down to a 4% composition using waste rock (Cameco Corp. 2009). This process generates significant amounts of uranium waste tailings, which by 2004 exceeded 36 million tons in the Athabasca Basin (Natural Resources Canada 2004). Uranium and metal mine tailings in general are characterized as being rich in potential contaminants to the groundwater system, such as arsenic (As), nickel (Ni), uranium (U) and radium (^{226}Ra) (Wolfaardt *et al.* 2008; Lee *et al.* 2008). For this reason, the

engineering of a containment facility is essential for maintaining toxic wastes segregated from the surrounding environment. The tailings management facility (TMF) (Figure 1.2) at Key Lake, Saskatchewan (also known as the Deilmann TMF) is an in-pit design for storage and disposal of the byproducts and wastes of the uranium milling process (Cameco Corp. 2009). The pit measures approximately 1000 meters by 600 meters with tailings depth of 60 meters on top of which sits a 45 meter layer of water (Cameco Corp. 2009).

The Deilmann pit was originally mined between 1989 and 1996, after which it was commissioned to store the remainder of the tailings from the Key Lake mill (Cameco Corp. 2009). The facility's envelope was lined with a modified bentonite, and the tailings consolidate in such a way that upon decommissioning, the groundwater will take the path

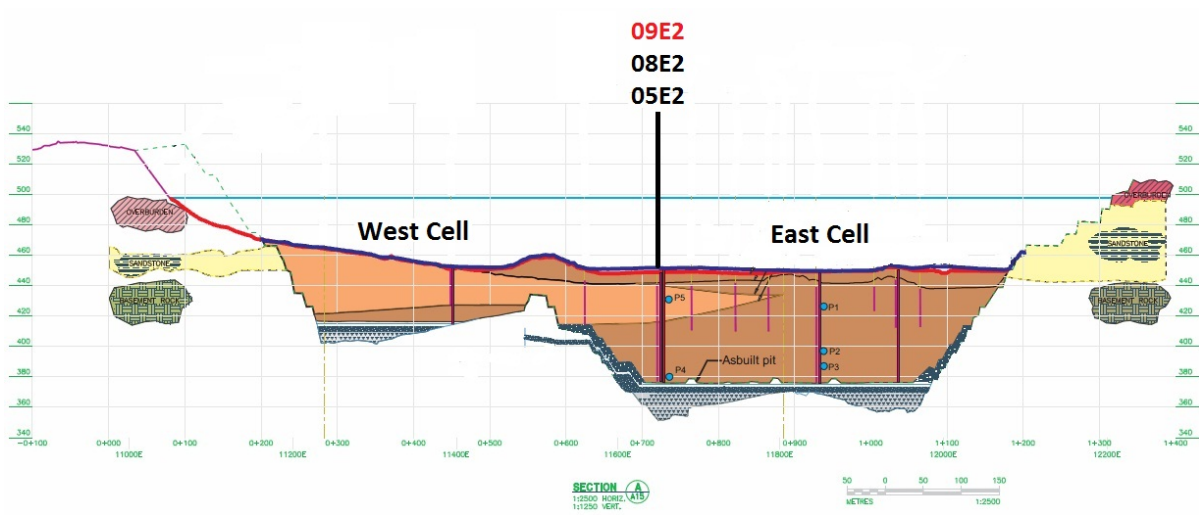


Figure 1.2. Cross-sectional area of the DTMF, showing depth variation and previous sampling points (adopted from Maathuis 2010).

of least resistance, around the DTMF (Cameco Corp., 2009). Due to significant consolidation, the hydraulic gradient between the tailings and the groundwater would be controlled by diffusion of the pore-waters rather than advection, thus further minimizing the contact between the elements of concern (i.e. heavy metals) in the tailings and the groundwater system. Managing the TMF consists of a two-step process involving containing the solids in their non-soluble form and treating the percolating water from the bottom of the pit to ensure no contaminants will reach the groundwater (Cameco Corp., 2009). The speciation of the specific solids is maintained by storing the tailings at a pH of 9-10, which in

the DTMF very rarely reach temperatures above 2-3°C (Appendix 1, Kotzer; direct communication).

1.2 Implications of Heavy Metal Chemistry

1.2.1 Iron in Anaerobic Environments: Valuable Microbial Energy Source

Iron is the fourth most abundant element in the earth's crust, representing 5.1% by mass (Straub 2001). In nature, iron is present under both trivalent (ferric iron) and divalent forms (ferrous iron), and forms stable complexes in both oxidation states (Kostka *et al.*, 1996, Straub *et al.* 2001). In the presence of oxygen, ferrous iron will only be stable under acidic conditions, otherwise quickly being oxidized to ferric iron (Viollier *et al.* 2000; Straub *et al.* 2001).

In sediments, soils as well as aquatic environments, iron minerals are not only very important in the biogeochemical cycling of organic compounds, major elements such as sulfur and phosphorous and trace elements such as heavy metals, but also the most abundant oxidants present in such environments (Kostka *et al.* 1996; Viollier *et al.* 2000). Because ferric iron forms complexes with organic acids and oxyhydroxide colloids, it becomes an optimum source for a microbial energy sink (Kostka *et al.* 1996; Viollier *et al.* 2000; Lloyd 2003). Iron (oxy)hydroxides undergo reductive dissolution as a cause of microbial metabolic activity by specialized bacteria, which is a process coupled with the oxidation of organic matter, however iron reduction could also take place as an abiotic process to a small extent in the presence of inorganic or organic reductants (Viollier *et al.* 2000).

In a natural setting, iron minerals appear in an amorphous or crystalline state, such as hematite, smectite and goethite, very rarely in a soluble state which is generally considered to have increased bioavailability (Kostka *et al.* 1996). Oxidized clay mineral particles, such as iron minerals, have larger lateral extents as well as a greater surface area, which provide suitable attachment substrates for microorganisms in sedimentary environments (Kostka *et*

al. 1996). The proximity between microbial cells and metal minerals, especially iron oxides and hydroxides, is very important for efficient metabolic activities (Lloyd 2003; DiChristina *et al.* 1994). The reduction of amorphous or crystalline iron minerals causes the collapse of the clay particles, increasing iron solubility and releasing other heavy metals associated with such complexes (Kostka *et al.* 1996; Beliaev *et al.* 1998).

1.2.2 Iron speciation and availability: A Function of Redox Potential and pH

The Eh is used as a numerical representation of the reducing or oxidizing strength of the particular redox couple and it is defined as the potential difference between the half element of the redox couple and the standard hydrogen electrode (Wimpenny *et al.* 1971; Rump 1999). Even though oxygen concentration and Eh are related (directly proportional to each other), measurements of Eh generally prove to be the more significant parameter (Jacob 1970). Oxygen plays an important role in subsurface sedimentary environments as well as water columns, acting as a regulator on the chemical make up of microorganisms as well as determining the type of organisms present through its concentration (Jacob 1970; Wimpenny *et al.* 1971). As pH values control the speciation of heavy metals as well as several other chemical processes at the microbial level, so does the Eh (Rump 1999). In water columns and sediments, anaerobic environments are characterized by low Eh values (Rump 1999). Table 1.1 shows the representation of Eh in millivolts as it pertains to various soil environments. Usually the upper layers of water columns or shallow water sediments will be aerobic due to oxygen diffusion, but as this oxygen gets depleted due to aerobic microbial growth, an oxygen gradient develops (Rump 1999). These basic principles can be applied to any flow system. If the Eh in an inoculated culture begins to decrease, this is evidence of microbial growth. Studies have shown that within 24 hours of inoculation with aerobic organisms in batch systems, the Eh decreased from +135mV to -280mV due to microbial growth (Jacob 1970).

Table 1.1. Scale of Redox Potentials and oxidation potentials measured with a platinum electrode. For the soil conditions given, the measurement is *in situ* (Adaptation from Jackson 2005).

Oxidation of Reduction Condition	Redox Potential or Eh (mV) most commonly used in soils and biological literature
KMnO ₄ in 1N H ₂ SO ₄	1500
Very well oxidized soil	800
Well oxidized soil	500
Moderately well oxidized soil	300
Poorly oxidized soil	100
Much reduced soil	-200
Extremely reduced soil	-500
Na ₂ S ₂ O ₄ (pH 8)	-600

Iron mineral speciation is affected by pH which in turn determines the reduction potential and ultimately bioavailability in terms of energy conservation (Thamdrup 2000). The pH dictates the speciation of iron oxides, having a more specific influence than other redox couples (Thamdrup 2000). This fundamental relationship between pH and redox potential is represented in Figure 1.3, which describes the change in iron speciation in coastal seawater. This image shows the gradual change from ferrous iron species to ferric iron species as the pH increases, and the gradual change from ferric to ferrous iron as Eh decreases, accompanied by increased solubility. The Eh of iron oxides increases by 59mV with every unit decrease in pH, meaning that more energy is available from iron reduction at lower pH values. Under these conditions, the reduction of iron minerals such as hematite and goethite can become much more favorable than for example sulfate reduction (Kostka *et al.* 1995; Postma *et al.* 1996).

The ferric/ferrous Eh is the strongest pH dependent redox couple when compared to other redox couples such as manganese, nitrate and sulfate (Thamdrup 2000). In a soluble chelated form, the Eh for the iron couple is close to +400mV. Thus soluble chelated iron is

slightly more thermodynamically favorable than the nitrate/ammonia redox couple (+380mV), but less favorable when compared to elemental iron (+760mV) which is very close to the Eh of oxygen (>800mV) (Thamdrup 2000). Ferrihydrites and ferric hydroxides have an Eh of ~0mV and -100mV respectively, which make these couples more favorable than sulfate (-200mV) (Thamdrup 2000), but can be considered as being non-labile species for microbial metabolic activity.

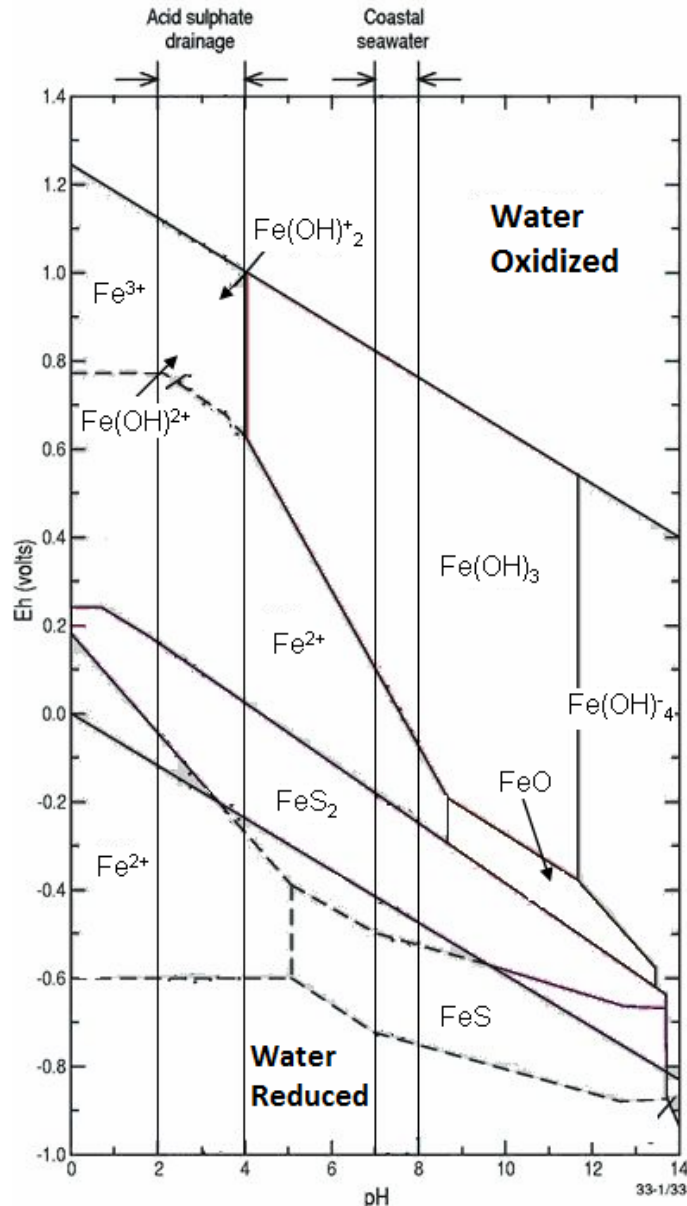


Figure 1.3. Stability field diagram for dissolved and solid forms of iron as a function of pH and Eh at 1atm and 25°C (Adopted from Elder 1988).

The classification of the Eh couples shows the importance of various ferric iron soluble and amorphous/crystalline complexes as potential energy sources for microbial growth in various environments. Overall, studying the fate of ferric iron in the presence of indigenous microorganisms will provide a good point of reference for studying other possible electron acceptors.

Although the presence of oxygen is essential for aerobic microbial growth, it also represses enzymes involved in the electron transport chain of anaerobic pathways. At various concentrations of oxygen in a system, separate physiological phases will occur, thus defining specific metabolic pathways which can be measured through the Eh. At an Eh value less than 0mV the Krebs's cycle enzymes, cytochromes and ATP pool are present in low concentrations and only hydrogenases are present at high levels (Wimpenny *et al.* 1971). At Eh values of +100mV cytochrome production is at a maximum and the ATP pool and cytochrome concentration start increasing also although oxygen is still barely detectable (Wimpenny *et al.* 1971). A range of +200mV and +300mV is representative of the optimal environment for TCA cycle enzymes and ATP pool with oxygen being easily measurable. Eh values above +300mV are marked by limiting conditions and decreased growth for facultative anaerobic organisms, due to slight toxicity of oxygen at such high concentrations (Wimpenny *et al.* 1971).

1.3 Arsenic: Co-precipitation and sorption to heavy metal complexes

The majority of mine tailings contain large concentrations of heavy metals such as copper, lead, gold and uranium (Lee *et al.* 2008; Lim *et al.* 2008). Complexed to these heavy metals, arsenic is considered to have a wide distribution in nature although it has a low abundance in the earth's crust (0.0001%), with average concentration of 2 μ g/g (Lee *et al.* 2008, Lim *et al.* 2008; Moldovan *et al.* 2008). Evidence suggests that although it is found in low concentrations, arsenic may have been of importance to early life on earth, presenting with an important source of energy generation by microbial activity (Oremland *et al.* 2009).

Arsenic is found in four different oxidation states: As(V) or arsenate which is the oxidized form, As(III) or arsenite which is the reduced form as well as As⁰ (arsenic metal) and As(-III) (arsine) (Lee *et al.* 2008; Lim *et al.* 2008). Arsenate and arsenite forms are a particular focus in research since these are most common in various environmental settings and important in biological nutrient and elemental cycling (Lim *et al.* 2008). Arsenic metal is very rare and arsine only exists in highly reduced environments (Lee *et al.* 2008). In environmental nutrient cycling, the particular redox reaction between arsenate and arsenite is very important in determining the mobility of this metal as well as toxicity, which makes it of significant interest in explaining cases of environmental contamination. Arsenite is approximately 200 times more toxic to biotic life compared to arsenate, and considerably more mobile in the natural water system, in the lower ranges of the pH scale (Ahmann *et al.* 1997, Lee *et al.* 2008; Oremland *et al.* 2009). A decrease in Eh will also render arsenic more mobile; generally in low Eh environments, representing anoxic conditions, the predominant form of arsenic will be As(III) (Ahmann *et al.* 1997; Lim *et al.* 2008). Otherwise, close to the recharge areas of groundwater aquifers or pore-waters, the predominant form is As(V), the more insoluble form (Lim *et al.* 2008). As(V)/As(III) Eh is measured at +130mV, which makes it a stronger oxidant when compared to sulfate/sulphide (-220mV) but significantly less than nitrate (+440mV) or oxygen (+818mV) (Oremland *et al.* 2009). Experiments performed on arsenic and selenium speciation in contaminated soils, have indicated that under an Eh of +500mV the majority of arsenic present was in an oxidized form, while Eh values of -200mV indicated significant increase in concentrations of reduced arsenic (Masscheleyn *et al.* 1991). It is also important to note that under low Eh conditions arsenate is present at low concentrations; however, it is thermodynamically unstable (Masscheleyn *et al.* 1991). These results correlate with the suggestion that microbial metabolic activity constantly influences the Eh, and heavy metals ultimately become sources of electron acceptors under anoxic environments, characterized by low Eh values.

Arsenic is generally concentrated in sediments, which is caused by two important chemical/physical properties: co-precipitation and sorption. Arsenate will co-precipitate with iron hydroxides, manganese and aluminum in anaerobic environments due to the sorption

capabilities to these complex species (Ahmann *et al.* 1997; Lee *et al.* 2008; Lim *et al.* 2008). These two concepts help explain arsenic solubility and explain what role iron hydroxides play in such processes in environmental settings (Ahmann *et al.* 1997; Niggermeyer *et al.* 2001). Amorphous iron complexes responsible for such interactions that are normally present in the environment are ferrihydrite, goethite, scorodite, magnetite and smectite (Cummings *et al.* 1999; Masscheleyn *et al.* 1991; Moldovan *et al.* 2008; Kostka *et al.* 1996; Straub *et al.* 2001). Although the trivalent (reduced) form of arsenic is much more mobile, both the pentavalent and trivalent forms sorb well to these species (Cummings *et al.* 1999). Other important abiotic factors that influence sorption properties are pH and As:Fe concentration ratio (Cummings *et al.* 1999; Niggermeyer *et al.* 2001). At low concentrations of arsenic compared to iron, at near neutral pH, arsenate sorption rates were shown to be slightly greater than arsenite the same observation being valid for the reverse scenario between As and Fe concentrations (Cummings *et al.* 1999). At higher pH, up to values of 10, the solubility of arsenic seems to be controlled by adsorption to ferrihydrite or amorphous aluminum hydroxide, which is most probably the case in the DTMF tailings phase (Moldovan *et al.* 2008) as well as the simulated flow-cell environment used in this study.

1.4. Microbiology of Metal Reduction

1.4.1 The Benefits of the Biofilm Matrix

Microorganisms in nature do not proliferate as individual cell colonies of pure cultures, but rather accumulate on surfaces and interfaces as polymicrobial aggregates such as biofilms (Amann *et al.* 1992; Flemming and Wingender, 2010). The biofilm is generally composed of an extensive and elaborate matrix of extracellular material produced by the organisms themselves, which connects and embeds the cells. The extracellular material is composed of different types of biopolymers known as extracellular polymeric substances (EPS), which are responsible for creating the three-dimensional scaffold of the biofilm as well as providing the requirements for surface adhesion and cohesion within (Flemming and

Wingender, 2010). Of the biofilm material, as little as 10% of the dry mass is comprised of the cells while the rest of 90% is the EPS matrix (Flemming and Wingender, 2010).

Bacterial cells that are part of a biofilm have a higher metabolic activity because of the many benefits of the EPS matrix, expression of adhesion-induced specific genes, and the opportunity for a greater number of bacteria to coexist and cooperate compared to free-floating cells (Bester *et al.* 2005; Flemming and Wingender, 2010). Under various environmental conditions, genes that express pili, flagella and surface adhesions have been involved in the formation of surface associated biofilms (Bester *et al.* 2005). EPS maintains cells in close proximity to each other, allowing for efficient intra-cellular communication as well as formation of a synergistic micro-consortium. The EPS matrix can serve as a source of nutrients for the embedded cells as it contains considerable amounts of nucleic acids, lipids and other biopolymers such as humic substance and represents a significant portion of the reduced carbon in soils, sediments and water columns. Components of lysed cells are maintained within this matrix and are available as a recycling system which could also be conceived as long term storage (Flemming and Wingender, 2010). Besides acting as a nutrient source, the EPS provides a suitable environment for bacterial proliferation and a protective layer against desiccation by allowing an increased rate of water retention, oxidizing and charged biocides, some antibiotics and metallic cations. At the same time the EPS provides sorption of organic compounds, enables enzymatic activity of exogenous macromolecules and promotes redox reactions through the large variety of electron donor/acceptor species present (Flemming and Wingender, 2010). Many natural populations can not be cultured through enrichments, thus explaining the limited characterization and understanding of environmental biofilm communities (Amann *et al.* 1992).

1.4.2 Microbial Iron Reduction in the Environment

Microbial metal reduction plays an important role in cycling of both organic and inorganic species in the environment by degradation of organic matter and influencing mineralogy by reductive dissolution processes of a wide variety of heavy metals such as As(V), U(VI) and Cr(VI) (Lloyd 2003). The most common metal species that experience

reduction in subsurface and interface environments are iron and manganese, in part because of higher concentrations in such environments and being the dominant electron acceptors, as well as the thermodynamic favorability mentioned earlier in which the Eh of the redox couples plays an important role (Cummings *et al.* 1999; Lloyd *et al.* 2003; Saltikov *et al.* 2005). Besides being the sole electron acceptor in some environments, iron is also a vital element of cellular components for all microorganisms and is required for the function of cytochromes and hydroperoxidases as well as nitrogenase activity (Hersman *et al.* 2001). In previous studies, Fe(III) concentrations below 0.1 μ M caused deprivation of many microbial species, thus demonstrating the importance of iron as a nutrient (Hersman *et al.* 2001). Although the capability of microbial metal reduction such as Fe(III) has been known for a very long time and may have been an early form of respiration on Earth, the link between redox transformations and energy production has only recently been delineated (DiChristina *et al.* 1994; Lloyd *et al.* 2003).

The dissimilatory process of metal reduction is recognized as being an important process in both pristine and contaminated sedimentary environments and is common among anaerobic organisms (Canfield *et al.* 1991; Lonergan *et al.* 1996). This metabolic pathway involves coupling the oxidation of a variety of short-chained fatty acids or aromatic hydrocarbons, such as toluene, phenol and benzoate, to carbon dioxide or smaller metabolic intermediates, while Fe(III) serves as a final electron acceptor (Lonergan *et al.* 1996; Beliaev *et al.* 1998; Gerlach *et al.* 2000; Lloyd 2003). Iron reducing bacteria are responsible for most Fe(III) reduction taking place in sediments, and often causes the release of other associated heavy metals such as As (Ahmann *et al.* 1997). Other microbial members of anaerobic communities which can reduce iron exist, such as the sulfate reducing bacteria, although their impact is assumed to be generally indirect through the production of hydrogen sulfide which chemically reduces Fe(III) (Ahmann *et al.* 1997).

1.4.3 Diversity among Iron Reducers

Fe(III) reducing organisms fall under two categories: those that completely oxidize multi-carbon compounds to carbon dioxide, and those that cause incomplete oxidation to acetate (Coates 1996). Most of the organisms attributed with such metabolic pathways are members of the *Proteobacteria* phylum with species such as *Shewanella*, *Pseudomonas*, *Geobacter* and *Desulfuromonas* and most of these organisms are either facultative or strict anaerobes (Loneragan *et al.* 1996; Lloyd 2003; Islam *et al.* 2004). The diversity of microorganisms that can cause such redox transformations is however much broader, extending from specialized organisms to other species such as archaea and fungi, which under various conditions can adapt various metabolic pathways (Lloyd 2003; Islam *et al.* 2004).

The *Shewanella* genus were originally discovered in 1988 and at that time it was characterized as *Pseudomonas* (Fredrickson *et al.* 2008). This genus currently holds 48 recognized species, which were found to have versatile anaerobic metabolic pathways being capable of transferring electrons to solid metal oxides as well as reducing sulfur (Fredrickson *et al.* 2008). These microbial species are attributed to abundantly populating redox interfaces, which would explain their metabolic diversity and ability to use non-standard electron acceptors such as chromium, uranium, tellurite and vanadate (Fredrickson *et al.* 2008). One of the most versatile iron reducers, which has been used extensively as a model organism, as well as in this study, in order to represent metabolic potential under various environmental conditions is *Shewanella putrefaciens*, a member of the γ -*Proteobacteria* group (DiChristina *et al.* 1994; Lloyd 2003). *S. putrefaciens* is a non-fermenting facultative anaerobe gram negative organism with a rod-shape morphology forming orange colored colonies, widely distributed in marine and freshwater sediments (DiChristina *et al.* 1994; Beliaev *et al.* 1998; Lim *et al.* 2008). This organism can use a wide range of organic and inorganic final electron acceptors, from metal oxides such as Fe, Co and Mn to fumarate, nitrate, thiosulfate and trimethylamine (Beliaev *et al.* 1998; Lim *et al.* 2008). Although capable of growing under both aerobic and anaerobic conditions as well as being able to sustain proliferation at a pH

range of 7-9, *S. putrefaciens* is restricted to using only small organic acids (acetate, propionate, butyrate, formate, lactate and ethanol) and hydrogen as electron donors (Ribet *et al.* 1995; Coates *et al.* 1996; Lim *et al.* 2008). This aspect seems to be generally true about all γ -*Proteobacteria* group members (Lloyd 2003).

Considering the close phylogenetic relationship between *Shewanella* and *Pseudomonas*, it could be expected that certain *Pseudomonas* species reduce Fe(III) for energy conservation since these too are facultative anaerobic organisms (Jones *et al.* 1983; Ribet *et al.* 1995; Lonergan *et al.* 1996; Islam *et al.* 2004). Past experiments have shown a 21% reduction in structural smectite by pure cultures of *Pseudomonas* in 14 days while other studies have shown *Pseudomonas* species being able to reduce selenium in coal mine tailings (Gates *et al.* 1993; Siddique *et al.* 2007). The microbial metal reduction pathway seems to be fairly similar regardless of the type of metal as it serves as final electron acceptor (Lloyd 2003). Although thought only to be able to use relatively labile forms of carbon for energy conservation, *Pseudomonas* species have been found to survive in crude oil environments while reducing Fe(III) (Obuekwe *et al.* 1982), a situation which is comparable with the DTMF environment.

Part of the δ -*Proteobacteria* group of iron reducers are the *Geobacter* species, which have also been extensively studied (Coates *et al.* 1996; Lonergan *et al.* 1996; Ahmann *et al.* 1997; Lee *et al.* 2008). *Geobacter metallireducens* is a strict anaerobic iron reducer which can couple the complete oxidation of multicarbon compounds to carbon dioxide, as well as aromatic hydrocarbons with the reduction of Fe(III) (Coates *et al.* 1996; Beliaev *et al.* 1998). This organism tends to dominate zones of Fe(III) reduction in subsurface environments with the ability to reduce other high valence metals as well with the notable exception of As(V) (Islam *et al.* 2004). *G. metallireducens* was actually the first organism described to utilize acetate and reduce iron, and was found to be closely related to the sulfate and sulfur reducer *Desulfuromonas acetoxidans* (Lonergan *et al.* 1996). Although sulfur reducing bacteria such as *Desulfuromonas acetexigens* and *Desulfuromusa kysingii* are also capable of Fe(III) reduction, these organisms cannot sustain growth with iron as the sole final electron acceptor (Lonergan *et al.* 1996). Other strict anaerobic organisms of interest include species of

Clostridium, which have been documented to reduce metals such as Fe(III), As(V) or U(VI) while fermenting organic matter (Lloyd 2003; Islam *et al.* 2004). *Clostridium beijerinckii* is another example of a strict anaerobe isolated from freshwater sediment with proven capability of reducing iron for energy conservation (Dobbin *et al.* 1999). The examples could also include species of *Micrococcus*, *Bacillus*, *Staphylococcus*, *Arthrobacter* and *Vibrio*, thus emphasizing the wide range of organisms reducing iron either for energy conservation, detoxification purposes or any other type of alternative metabolic pathway in a variety of environments (Jones *et al.* 1983). Although this redox metabolic pathway includes a wide range of bacteria and archaea as well as extremophiles such as thermophiles and acidophiles, the distribution patterns for iron reducing organisms in the environment are not yet fully understood (Lloyd *et al.* 2003).

1.4.4 Redox Metabolic Activities

Microbial metabolic activity in anaerobic environments can be explained by the central concept of oxidation and reduction, a chemical reaction which does not involve oxygen as the final electron acceptor, but rather other inorganic or organic species (Lonergan *et al.* 1996; Panak *et al.* 1998; Lloyd 2003). Microbial metabolic pathways can also be categorized as having a direct or an indirect impact on the surrounding environment, by changing chemical speciation through changes in pH and Eh, as well as bioaccumulation or biosorption of various heavy metals (Panak *et al.* 1998). Such interactions between microbes and cycling of solutes are common processes in metal mine tailings and form the basis for bioleaching processes (Panak *et al.* 1998; Lee *et al.* 2008). The reduction of various metals in anaerobic environments can also be a good example of microbial adaptation. The change in reduction of one metal to another shows the adaptation of microbial respiratory pathways in sediments which is expressed through dynamic changes in a mixed microbial community (Islam *et al.* 2004). Certain members of a microbial community could be active, depending on nutrient available or altering the metabolic pathway by modifying the expression of a relevant reductase, proven in past experiments of iron and As(V) reduction impacts on groundwater systems (Islam *et al.* 2004).

The metabolic rate of iron reduction is highly dependent on the proximity between the microbial cell membrane and the metal oxide (Beliaev *et al.* 1998). Since this redox reaction is essentially the transport of electrons from a donor to an acceptor across an electron transport chain, the faster the electrons are transferred to the final acceptor the more efficient is the respiration process. This theory has been proven in past experiments that have shown the iron reduction process to be absent upon separation of the cells from the oxide particles (Beliaev *et al.* 1998). Figure 1.4 represents direct and indirect reduction of iron minerals as a metabolic cycle and relationship between energy conservation and cellular attachment to final electron source (Lloyd 2003).

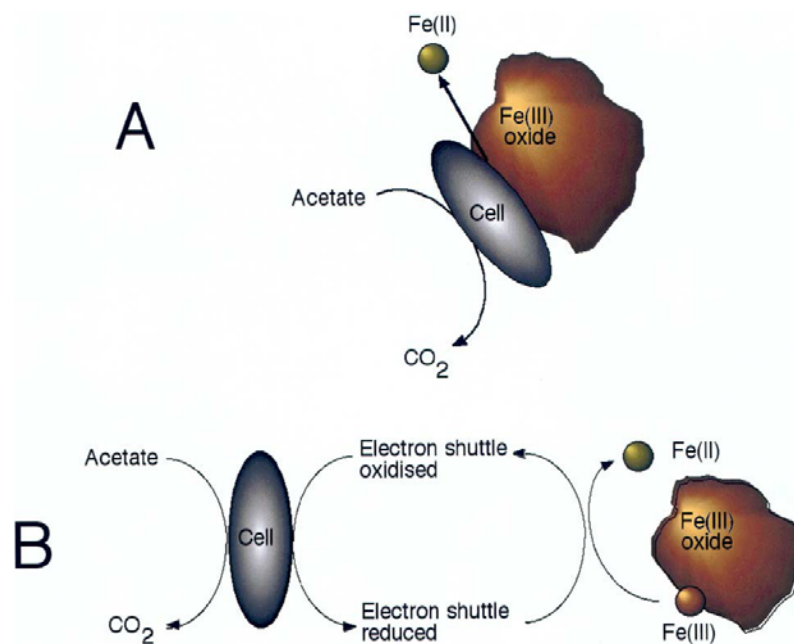


Figure 1.4. Mechanisms of iron reduction via direct (A) and Indirect (B) (mediated) methods (Adopted from Lloyd 2003).

Microbial attachment to ferrihydrite and ferric hydroxides is important, specifically because clay minerals provide one of the most catalytic surfaces in sedimentary environments (Kostka *et al.* 2002). This same observation was made for pure cultures of *Shewanella*,

Pseudomonas and *Geobacter* (Beliaev *et al.* 1998; Lloyd *et al.* 2003; Lim *et al.* 2008). In studies done specifically on *G. metallireducens*, the cells were determined to synthesize pili when grown on insoluble forms of iron or manganese minerals emphasizing that cellular attachment to the final electron acceptor substrate is an essential aspect of microbial metal reduction (Lloyd 2003). This aspect could be relevant to biofilm formation in the DTMF environment

Reduction of iron clays and minerals is not only influenced by microbial numbers present but also by environmental physical characteristics such as pH (Lim *et al.* 2008). Amorphous and crystalline forms of iron have an optimum near-neutral reduction pH (5-6), and the metabolic rate will decrease with increasing pH above 6 (Kostka *et al.* 1996). However, even with increasing pH values of 5-9, literature shows that microbial metabolic rates remain significantly high, at temperatures ranging from 6-60, proving that organisms will eventually adapt to changing environmental conditions and maintain steady proliferation (Kostka *et al.* 1996). The form and availability of iron in the environment will determine growth patterns, metabolic activity and chemotactic movement (Kostka *et al.* 2002; Saltikov *et al.* 2005). Under epifluorescence microscopy, cell sizes were determined to be significantly larger when the cultures were grown in the presence of soluble rather than solid forms of iron. This could be explained by an increased bioavailability of iron in the aqueous form compared to amorphous or crystalline iron (Kostka *et al.* 2002). Metal reducing microorganisms can move in the direction of high metal ion concentration areas, towards the soluble products of metal reduction by chemotaxis (Saltikov *et al.* 2005). This could explain the increased sensitivity of strains *G. metallireducens* and *Shewanella* ANA-3 to Fe(II) and As(III) respectively (Saltikov *et al.* 2005).

The electron transport chain for iron reduction is still not well understood, however it is evident that cellular outer membrane putative c-type cytochromes are involved and play a crucial role in anaerobic respiration of specialized species such as *Shewanella* and *Geobacter*, although the terminal reductase has yet to be identified (Coates *et al.* 1996; Lloyd

et al. 2003; Fredrickson *et al.* 2008). The c-type cytochromes distribution in the outer membrane can be seen in Figure 1.5, in *S. oneidensis* tagged cells (Lloyd 2003).

In pure cultures of *S. putrefaciens*, colonies lose their pigmentation and their redox metabolic ability when starved for iron (Beliaev *et al.* 1998). The c-type cytochromes present in the outer membrane thus rely on a specific concentration of Fe(III) for constant metabolic activity, as mentioned earlier (Beliaev *et al.* 1998). The activity of the cytochromes is dictated by other final electron acceptors present. These proteins can become completely inactivated by the presence of oxygen, while nitrate will only partially inhibit metal reduction pathways (Lloyd 2003).

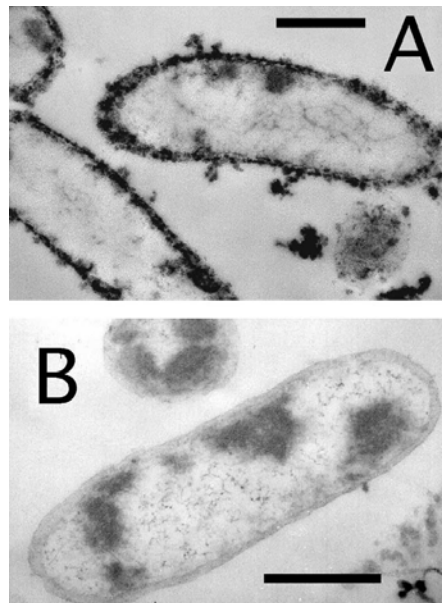


Figure 1.5. Transmission electron micrograph showing the distribution of c-type cytochromes in the outer membrane in *S. oneidensis* (A) and *Pelobacter carbinolicus* (B) cell lacking such cytochromes (Adopted from Lloyd 2003).

This sensitivity to surrounding chemical species could explain variations in metabolic pathways of facultative anaerobic organisms. Studies have shown that *S. putrefaciens*, although originally thought not to be able to respire iron under aerobic conditions, will eventually begin reducing iron once it depletes all oxygen present and reverts its metabolism

to metal respiration for energy production (DiChristina *et al.* 1994). This proves that prolonged exposure to oxygen will not permanently inhibit iron reduction for this organism.

Microbial metal solubilization and reduction could also occur for reasons other than energy conservation, such as growth requirements by solubilizing Fe(III), as a detoxification pathway in the case of As(V) or as an indirect method of metal reduction (Hersmann *et al.* 2001; Lloyd 2003; Lee *et al.* 2008). Cultures of *Pseudomonas mendocina* were capable of growing aerobically on insoluble sources of iron such as goethite, ferrihydrite and hematite while releasing Fe(III) for growth purposes (Hersmann *et al.* 2001). This metabolic pathway seems to be mediated by siderophores or extracellular ligands which are used by cells to capture Fe(III) directly from Fe(III) hydroxides causing dissolution (Hersmann *et al.* 2001). Not only were these processes efficient enough to acquire Fe(III) for the cells attached to the solid phase Fe(III) minerals, but this metabolic activity began supplying the planktonic cells with enough Fe(III) to maintain growth (Hersmann *et al.*, 2001).

As(V) is an important element of many subsurface sedimentary environments, since its solubilization causes contamination of drinking water supplies which can lead to poisoning of epidemic proportions (Saltikov *et al.* 2005). Currently there are 20 microbial known species known to be capable of reducing As(V) through a dissimilatory process, and these are mostly facultative anaerobic heterotrophs (Oremland *et al.* 2009). Considering that chemical arsenic reduction in anoxic environments takes place at a very slow rate, often considered insignificant due to overall equilibrium, there are two biotic mechanisms by which arsenic gets reduced in sediments and soils: reduction and dissolution of iron hydroxides associated with arsenic by iron-reducing microorganisms, and direct reduction of arsenic whether associated to other metal complexes or free-floating form of As(V) by specialized arsenic reducing microorganisms (Ahmann *et al.* 1997; Cummings *et al.* 1999; Oremland *et al.* 2009). Although microbial reduction of iron hydroxides is an important and frequent process in anoxic environments, the solubilization of associated arsenic is a slow process (Masscheleyn *et al.* 1991). One example of a stepwise microbial iron hydroxide reduction / solubilization of arsenic was documented in Bangladesh, where the groundwater

aquifers have been extensively contaminated (Mladenov *et al.* 2010). The involvement of bacterial growth in As(V) reduction is an ancient process, dating from primordial Earth which made its way among prokaryotic species through gene transfer and divergent evolution (Oremland *et al.* 2009). As(V) is considered an analogue of HPO₄, and as such possesses structural similarities (Saltikov *et al.* 2005). During the process of HPO₄ uptake by bacterial cells, As(V) will enter the cells via low-affinity pumps (Saltikov *et al.* 2005; Lee *et al.* 2008). Once As(V) reaches toxic levels in the cytosol, As(V) is reduced to As(III) with the concomitant oxidation of thiols (Saltikov *et al.* 2005; Lee *et al.* 2008). The increased solubility and as a result the mobility of As(III) will cause it to be excreted out of the cytosol, via membrane efflux pumps, and into the surrounding environment (Saltikov *et al.* 2005; Lee *et al.* 2008). This process can take place under both aerobic and anaerobic conditions and is regulated by the *ars*-operon, a well studied system in many bacteria and archae, including less specialized organisms such as *Escherichia coli* and *Staphylococcus aureus* (Saltikov *et al.* 2005; Lee *et al.* 2008). A second metabolic pathway for As(V) reduction exists for energy conservation purposes (Saltikov *et al.* 2005; Lee *et al.* 2008; Oremland *et al.* 2009). Many organisms that have such abilities are known Fe(III) reducers because Fe(III) minerals are much more abundant and very good scavengers of other heavy metals, such as As(V) (Chao *et al.* 1972; Lloyd 2003; Lee *et al.* 2008). The As(V) dissimilatory microbial reduction is regulated by the *arr*-operon, a loosely understood system. The *arr*-operon is only activated under anaerobic conditions, since this is an energy conservation process, however, immediately inhibited by the presence of nitrate (Saltikov *et al.* 2005). The *ars* and *arr* operon systems interchange; the first depending on the degree of solubility of As(V) and whether it is adsorbed onto metal oxides, and the latter depending on aerobic or anaerobic conditions and availability of As(V) (Saltikov *et al.* 2005). The known iron reducer *G. metallireducens* was found not to be able to reduce considerable amounts of As(V) from ferric arsenate when compared to sediment microcosms, suggesting that *in-situ* conditions might be characterized as a series of metabolic pathways leading to Fe(III) and As(V) reduction (Ahmann *et al.* 1997). However, other Fe(III) reducers that can express the As(V) reductase exist, such as *Wolinella succinogenes* and *Geospirillum barnesii* as well as 5

different species of *Shewanella* and 2 species of *Geobacter* (Cummings *et al.* 1999; Oremland *et al.* 2009).

Sulfate reducing bacteria are also important organisms in anaerobic sedimentary environments (Canfield *et al.* 1991; Lonergan *et al.* 1996). These organisms are associated with the indirect reduction of Fe(III) and As(V) by production of hydrogen sulfide which chemically reduces Fe(III) or simply by reducing the pH which changes metal speciation (Ahmann *et al.* 1997; Cummings *et al.* 1999; Viollier *et al.* 2000). Other sulfate-reducers, such as *Desulfotomaculum auripigmentum*, can perform As(V) reduction through a dissimilatory pathway (Ahmann *et al.* 1997). Some organisms adapted to survive in such environments reduce Fe(III) and As(V) metals for energy conservation indirectly by producing organic molecules acting as electron shuttles (Lloyd 2003). Humics and other extra-cellular quinones can transport electrons from the outer membrane of the bacterial cell to the surface of the metal, experiencing a redox reaction itself (Lloyd 2003). Part of extra-cellular organic components that bacterial cells produce is the EPS network mentioned earlier, which could also decrease the environmental pH at a microcosm level, which could impact metal speciation and cause solubilization of Fe(III) and As(V) chemical species (Lee *et al.* 2008).

Literature shows that heavy metal solubilization is a dominant process in subsurface sedimentary environments under anaerobic conditions. Fe(III) reduction is clearly one of the most common methods for energy conservation by microbial activity and these activities have been documented to impact the geochemical aspect of these environments. Fe(III) insoluble complexes are some of the most abundant chemical species in soils and sediments, and often found to be associated with other heavy metals such as As, due to ferrihydrite and Fe(III) (hydr)oxide affinity for such metalloids. Redox reactions associated with microbial metabolic activities will cause solubilization of both Fe(III) complexes as well as any associated metals such as As, either through direct metal reduction by specialized microorganisms or through a series of metabolic pathways that complement each other. Such biochemical processes are of concern for uranium mine tailings due to the possibility of

incremental release of toxic heavy metals, however the impact of microbial activity on the bulk tailings body over an extended period of time is not yet known.

CHAPTER 2: METHODOLOGY

2.1 Site location and site description

The Deilmann Tailings Management Facility is located in close proximity to the uranium mill at Key Lake, Saskatchewan. The uranium waste tailings are pumped subsequently in the Deilmann pit, which has an elongated shape, divided in two cells: the east and the west (Maathuis 2010). Once the entire pit had been mined out by 1999, a bottom drain was constructed and is used to pump percolating water back to the surface for re-treatment (Maathuis 2010). This drain also has the purpose of consolidating water and groundwater (Maathuis 2010). Geochemical and geotechnical analyses have taken place at the DTMF since 1997 through a number of field studies including drilling investigations for deep tailings sediment sampling (Maathuis 2010). In 2001, 2002 as well as 2010 interface tailings samples were taken using clam samplers (Maathuis 2010).

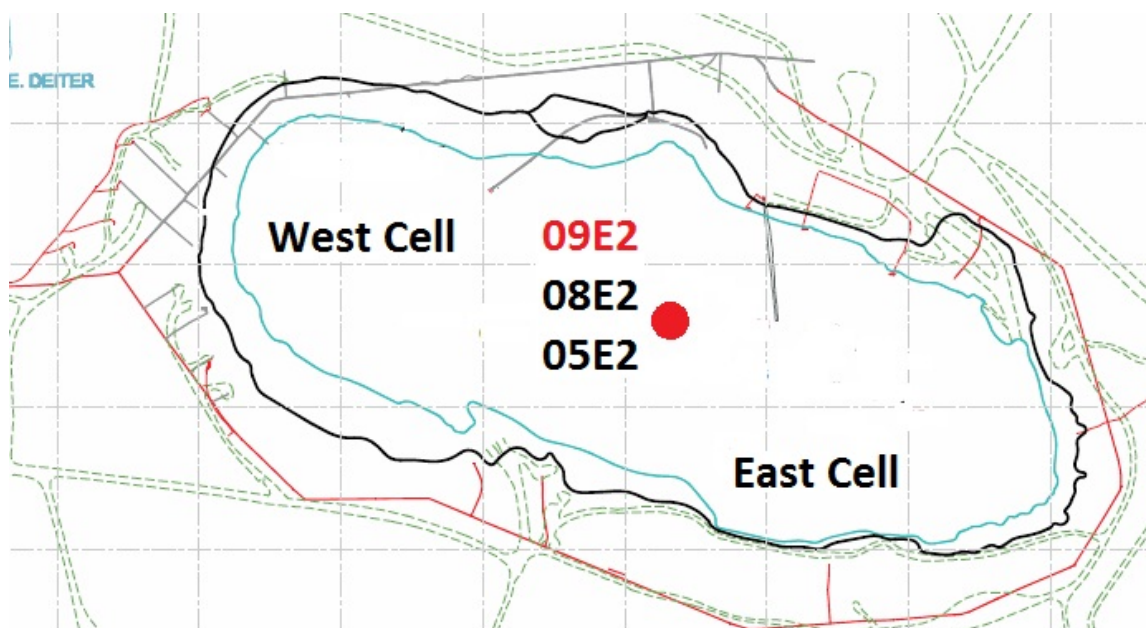


Figure 2.1. Locations of the 2005, 2008 and 2009 boreholes and monitor wells; the large red marker represents the location of this study's sample location (E2 borehole).

The DTMF sampling points have been strategically chosen according to proximity to the discharge pipes as well as previously characterized locations to monitor tailings physical and chemical parameters. The 2009 drilling location, shown in Figure 2.1 (E2 borehole) is one area that has been sampled in the past (1999, 2005 and 2008) (Maathuis 2010).

2.1 Core Sampling

The tailings body was sampled using a sonic rig mounted on a barge. Core samples were obtained using a 3.42 m long flow-through core barrel with a 5.08cm diameter. The tailings body was sampled vertically using 3 meter drill stem lengths. The cores were subsampled into plastic sleeves, for various physical analysis such as pH, redox potential, dissolved oxygen and temperature. Due to the soft and inconsistent nature of the tailings within the first 4.2 meter, no samples were collected at that depth. The sampling site was chosen according to previous knowledge of chemical measurements as well as previous drilling exercises (Maathuis 2010).

From the initial core samples, sediment subsamples were aseptically collected in duplicates for microbial analysis according to type of incubation (i.e. aerobic and anaerobic) and three samples for each type of incubation for a total of 6 samples per core using 10mL BD sterile syringes (VWR[®] Canada) which were previously modified by removing the Luer-Lok tip. The syringe subsamples were placed in sterile Whirl-Pak bags, which were sealed to contain moisture and to avoid contamination. The anaerobic incubated samples were stored under O₂-free atmosphere by purging with N₂ gas (grade 4.8) and maintained anaerobically using GasPak catalyst sachets (VWR[®]), in an anaerobic vessel. All samples were refrigerated during transport and storage. The initial tailings cores were characterized analytically in terms of pH, redox potential, dissolved oxygen and temperature. The analytical measurements taken on the core samples were performed at the same locations as the microbiological sub-sampling.

2.2 Bacterial Culturing

All anaerobic bacterial culturing procedures were performed in an anaerobic chamber (Coy Laboratories, Type B Vinyl Anaerobic Chamber), with gas composition of 7.5% H₂, N₂ balanced without CO₂, in order to avoid pH interference. All media were made with distilled water, unless otherwise specified. For enrichment purposes, 0.2 g of tailing material from each sub-sample was added directly to different types of media with variations in pH and nutrient content. The default growth medium used was 10% Luria-Bertani (LB) normal salt concentrations at neutral pH (Table 2.1). The growth medium was used because it contained a variety of electron donors and acceptors; it was autoclave sterilized and incubated aerobically at room temperature.

Table 2.1. LB Aerobic Medium used for enrichment purposes.

Luria-Bertani (LB) Normal Salt Media	
Component	Concentration (g/L)
Peptone	10
Yeast Extract	5
Sodium Chloride	5

In addition to enriching with LB medium, ferric citrate anaerobic medium was used at both neutral and alkaline pH (Table 2.2). The pH of the medium was buffered using a mixture solution composed of sodium carbonate/bicarbonate, pH 10.14 (Delory 1945). A 0.1M sodium carbonate solution (10.599 g/L) was prepared as well as 0.1M sodium bicarbonate (8.4 g/L), which were then mixed in a 3:2 (Na₂CO₃:NaHCO₃) volume ratio to achieve the desired pH. The buffer solution was added drop-wise to the medium until a pH values of 7.0 (neutral pH) and 9.5 (alkaline pH) were reached. The medium was autoclave sterilized, purged with N₂ gas (Lidle, Grade 4.8) for approximately one hour, and stored in the anaerobic chamber.

Table 2.2. Anaerobic Ferric Lactate Medium used for flow system and enrichment purposes.

Ferric Lactate Anaerobic Media			
Component	Concentration (g/L)	Ferric Iron Concentration	Lactate & Citrate Total Carbon
Ferric Ammonium Citrate	1.224	5.0mM	0.9g/L
Sodium Lactate	1.525		
Yeast Extract	0.250		

For the initial enrichment with ferric lactate medium, the 0.2 g tailings material was added in a 15 mL Falcon tube (BD Biosciences, 352096) and incubated for two weeks. Two subsequent enrichments were performed by inoculating 10 mL of the same medium in anaerobic serum vials with a 1 mL aliquot of enrichment. These enrichments were used as inoculum source for the flow-cell system.

2.3 The Flow-cell system

In order to study microbial community growth in a dynamic system with constant nutrient input, a flow-cell system (Bester 2008) was used. Figure 2.2 shows the design of the flow-cell chamber. The flow cell body was constructed using rectangular segments of plexiglass (8.0 cm x 5.0 cm x 1.5 cm). Using a Sherline 5400 milling machine (Sherline Products) with a Sowa M42 drill bit (0.3 cm diameter), a rectangular chamber (4.5 cm x 3.0 cm x 0.8 cm) was carved in the middle of the plexiglass segment. Inlet and outlet ports were drilled using a 0.3 cm diameter drill bit. The flow-cell was sterilized by immersion in 20% hypochlorite solution for 24 hours and autoclaving before assembly.

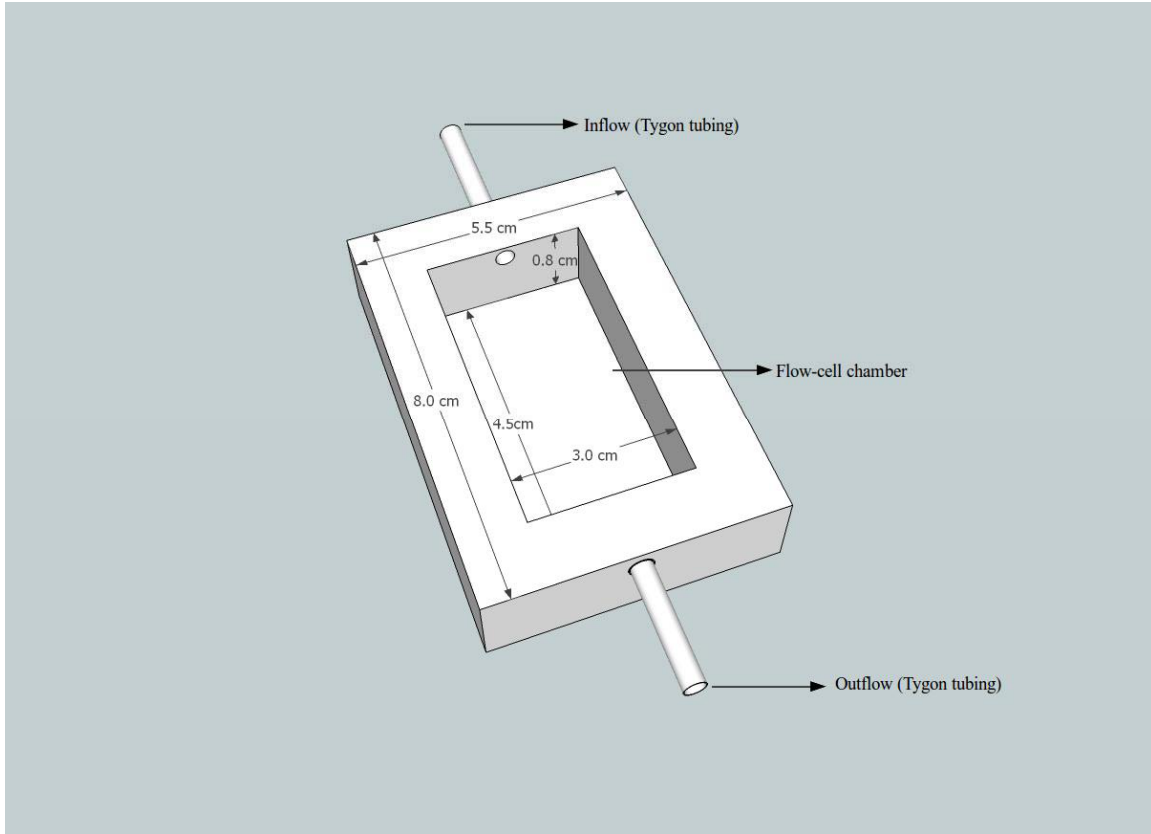


Figure 2.2. Design of the Flow-cell housing and chamber, constructed from an 8.0 cm x 5.5 cm x 1.5 cm block of plexiglass.

The flow-cell chamber was then packed with a combination of kaolinite clay ($\text{Al}_2\text{Si}_2\text{O}_5(\text{OH})_4$) (Jefferies 1988) and rock sand (obtained from local hardware store). The two components were mixed with water until a 5:2:1 (clay: sand: water) ratio was obtained and the resulting mixture was autoclaved. This mixture was packed in to the flow-cell chamber in a laminar hood and used as the attachment substrate. Depending on the purpose of the flow-cell experiment, the flow-cell chamber was sealed using GE all purpose 100% silicone glue either with a thin piece of plexiglass for analytical measurements or with a microscopy cover slip (4.8 cm x 6.0 cm) (Gold Seal, model 3334) for microscopic measurements. The space between the cover and the attachment substrate was approximately 1 mm, with a calculated volume of 1.350 mL (1350 mm^3). Figure 2.3 shows assembled sterile and running flow-cells.

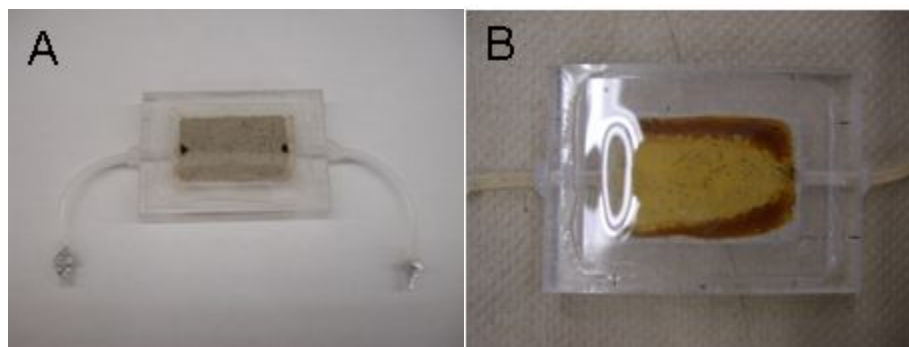


Figure 2.3. Representation of a packed sterile flow-cell (A) and a flow-cell connected to the flow system (B), packed with attachment substrate.

The flow-cell chamber ports were fitted with Tygon® tubing, with an internal diameter of 0.158 cm, (VWR Scientific, 63010-009), sealed with silicone glue and fitted with regular barbed straight connectors, at the opposite end, with the same internal diameter. All tubing and connectors were autoclaved. Once the components of the flow-cell were assembled, 30 minutes of UV radiation was used for further surface sterilization.

Figure 2.4 shows a schematic of the flow-cell system. The same type of autoclaved Tygon® tubing was used throughout the entire flow system, as this material does not allow significant gas exchange with the surrounding environment.

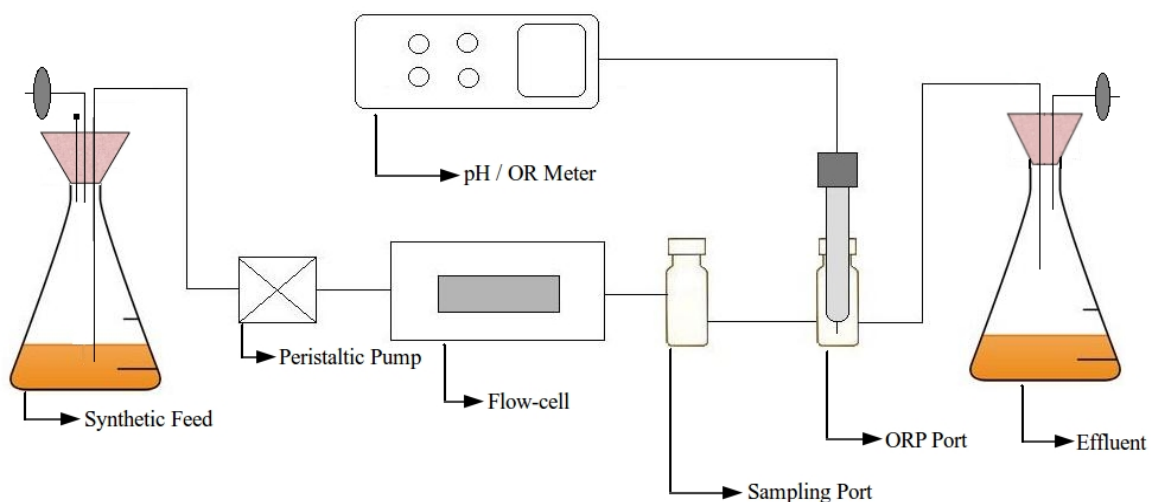


Figure 2.4. Schematic of the anaerobic continuous flow system created to study microbial metabolic activity, showing the major components.

The system consisted of synthetic feed pumped from the partially-sealed medium flask with a Watson Marlow 8-channel peristaltic pump (205S/CA low flow multi-channel pump) at a rate of 16.6 cm/hr (5 mL/hr) at the clay/liquid interface to achieve a flow rate as close to diffusion as possible. The system was fitted with a sampling port upon exit from the flow-cell chamber, as well as an oxidation-reduction probe (ORP) (VWR® Symphony® glass combination redox electrode, 14002-858) located after the sampling port. The sampling port consisted of a modified 5 mL serum vial, fitted with inlet and outlet ports and crimp sealed with a rubber septum (1 cm x 1 cm). The ORP port consisted of a similar modified serum vial, in which the probe was fitted using silicone tubing (internal diameter 1.8 cm) and sealed with Tygon tubing around the glass body of the probe (inner diameter 1.2 cm). The probe was connected to a pH/OR portable meter (VWR® Symphony® SP70P, 11388-326) for continuous readings. A partially-sealed sterile effluent flask was located downstream the ORP port.

Table 2.3. Ferric Lactate medium used for nutrient poor flow-cell experiments.

Ferric Lactate Anaerobic Media #2			
Components	Concentration (g/L)	Ferric Iron Concentration	Lactate & Citrate Total Carbon
Sodium Chloride	0.5000	5.0mM	20mg/L
Sodium Citrate	0.0297		
Sodium Lactate	0.0310		
Yeast Extract	0.0500		
Ammonium Chloride	0.1000		
* Ferric-NTA*	50mL soln. / L		
* Ferric - NTA Preparation			
Ferric Chloride 6H ₂ O	2.7 / 100mL	Ferric Iron Concentration	
Disodium NTA	2.35 / 100mL	100mM	
Sodium Bicarbonate	1.64 / 100mL		
NTA = Nitritotriacetic Acid			

The synthetic feed pumped through the system was initially constituted of the same components used in the enrichment step: ferric lactate medium at the similar nutrient concentrations (total lactate/citrate carbon concentration of 0.9 g/L, Table 2.2). These first sets of experiments were meant to describe microbial metabolic rate under favorable

environmental conditions for ferric iron reduction. For the second set of experiments, an oligotrophic (nutrient poor) synthetic feed was used (Table 2.3), with a lactate/citrate carbon concentration of 20 mg/L, made up of 10 mg/L lactate and 10 mg/L citrate. This level of carbon is comparable to the dissolved organic carbon concentrations (10-20 mg/L) detected in the *in-situ* pore-waters of the tailings system (Maathuis 2010). The amount of yeast extract added would comprise an insignificant amount of organic carbon, but rather only added to supply essential vitamins. Ferric iron concentrations were maintained at 5mM in order to assess the impact of carbon deprivation on metabolic activity. In order to maintain iron in a soluble state and stable enough to withstand precipitation due to autoclave sterilization, ferric nitrilotriacetic acid (NTA) was used. For the nutrient poor flow-cell experiments, the synthetic feed was buffered to a high pH (9.5) with phosphate buffer at pH 11.5, prepared by adding 5M NaOH drop wise to 0.05M KH_2PO_4 , until the desired pH was reached.

In both cases, the media was made in 2 L Erlenmeyer flasks and sealed with rubber stoppers, also described in Figure 2.5, containing three ports: 0.2 μm Millex autoclavable air filter to maintain equal flask headspace pressure inside the anaerobic chamber, one vent port to release pressure during autoclaving and the outflow port connecting the Norprene tube inside the flask with the flow system Tygon® tubing.

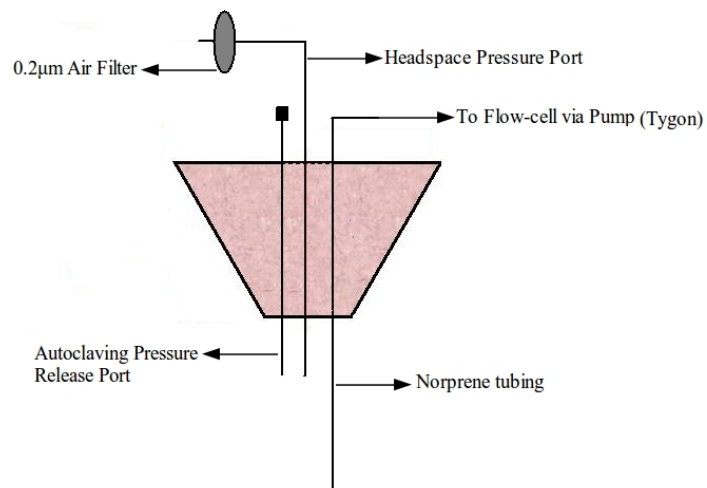


Figure 2.5. Illustration of the modified rubber stoppers used to seal the synthetic feed flasks and maintain their sterility and anaerobic condition; only the headspace pressure and flow-cell ports were closed during autoclaving; only the headspace pressure port was closed during N₂ purging; only autoclaving pressure release port was closed while running the flow system.

The medium was autoclave sterilized. After sterilization and while it was still hot, the medium was purged with N₂ gas directly into the liquid for one hour, before being transferred into the anaerobic chamber and connected to the flow system.

2.3.1 Flow-cell Inoculation

Negative control flow-cells were not inoculated and were maintained sterile by the addition of sodium azide to the synthetic feed (final concentration of 1 mg/L). Positive control flow-cells were inoculated with pure culture *Shewanella putrefaciens* (ATCC BAA-1097™), generously provided by Dr. Korber from the University of Saskatchewan. Sample flow-cells were inoculated with mixed communities previously enriched, either at neutral or high pH (depending on experiment) in order to maintain similar growing environments and shorten time of adaptation. For both positive control and sample flow-cells, the inoculation was done by injecting 1 mL volume from culturing vials, using sterile 1 mL syringes and 25 G needles, through the Tygon® tubing immediately at flow-cell chamber entrance. The punctured tube was sealed off using silicone glue, after which the system's flow rate was shut off for 30 minutes to facilitate microbial attachment to the kaolinite clay and sand surface.

2.4 Analytical Analysis

2.4.1 The FerroZine Method

For the analytical determination of ferrous iron concentration, the colorimetric FerroZine method was used (Viollier 2000), which is a slightly modified protocol, although based on the same principles developed by Stookey (1970). The ferrozine reagent (monosodium salt hydrate of 3-(2-pyridyl)-5, 6- diphenyl- 1, 2, 4- triazine- p,p' -disulfonic acid) reacts with divalent iron to form a stable magenta complex.

All reagents in this method were prepared in acid-washed glass bottles/containers, using mili-Q water (18.2M Ω ·cm). Sampling of the flow-system was performed daily for the duration of each experiment. The samples were collected through the sampling port, using sterile 1 mL syringes and sterile needles. A sample volume of 950 μ L was added to 50 μ L concentrated HCl (final concentration of 0.5N HCl), to stabilize ferrous iron under aerobic conditions. This mixture was gently vortexed and stored at 4°C in 2 mL Eppendorf tubes until analysis.

For the colorimetric reaction, ferrozine reagent (0.01M) was prepared in 0.1M ammonium acetate and the buffer solution was prepared by adding 38.54 g ammonium acetate in 60mL mili-Q water, buffered to pH 9.5 with 1.0M NaOH to a final volume of 100 mL. The ferrous iron standards were made from a 1L stock solution of FeSO₄·7H₂O (100 mg/L) prepared in 0.5M HCl, as per Table 2.4.

Table 2.4. Preparation of Ferrous iron standards for the FerroZine colorimetric method.

Volume From Stock (mL)	0.5M HCl added	Final Fe(II) Concentration (mg/L)
2.5	97.5	2.5
5	95	5
7.5	92.5	7.5
10	90	10
12.5	87.5	12.5
15	85	15
17.5	82.5	17.5
20	80	20
23	77	23

Using Sarstedt 10mm cuvettes (1.5 mL volume), the components were mixed in this exact order for the reaction procedure: 750 μ L mili q water, 100 μ L sample, 100 μ L ferrozine and 150 μ L buffer solution. The color was allowed to develop for 5-10 minutes after which colorimetric measurements were taken at 562nm using a Perkin Elmer Lambda 20 UV/VIS spectrophotometer. Both samples and standards readings were completed in triplicate. In order

to measure ferrous iron concentrations in samples of mixed community and pure culture, 5 and 15 fold dilutions, respectively, were necessary to maintain values within the range of absorbances recorded for the standards.

2.4.2 OR probe preparation and data recording

The OR probe was cleaned, sterilized and calibrated before every set of experiments. The cleaning procedure involved immersing the probe in a 0.1M HCl solution for 30 minutes, as well as draining and refilling the glass body with the internal reference solution (AgCl). The probe was then re-calibrated using ORP Standard solution (Thermo Scientific) based on the relative redox potential of the standard solution, the specifics of which are summarized in Table 2.5 below. The probe was sterilized by immersing it in a 1:10 hypochlorite solution for 30 minutes, after which it was fitted in the already sterilized glass T-connector mentioned earlier.

Table 2.5. Relationship between Relative Eh and Absolute Eh required for ORP calibration.

Temperature (°C)	Relative Eh Value (mV)	Absolute Eh (mV)
20	424	219
25	420	220
30	415	220

OR values were recorded at 1 hour intervals over the duration of the flow-cell experiment. The values were stored onto the portable pH/OR meter and were retrieved using a COM-port connection to a computer through Windows HyperTerminal.

2.5 Microscopy

2.5.1 Confocal Laser Scanning Microscopy (CLSM)

For confocal laser scanning microscopy a Nikon Digital Eclipse C1si system with 20X, 40X and 60X-oil immersion objectives was used. Images were taken using the 488nm laser for excitation, but better three dimensional details were acquired using epifluorescence microscopy. The flow-cells used for CLSM purposes were sealed using a regular cover slip, to accommodate the short focal length of the microscope's objectives (1.0 mm, 0.12-0.15 mm and 0.13 mm respectively). After running the flow-cell for 8 days in order to allow a significant amount of biofilm formation, the flow-cell was injected with SYTO[®] 9 green fluorescent nucleic acid stain (Invitrogen[™]) through the inflow Tygon tubing, as per indications in Table 2.6 below.

Table 2.6. Description of procedure for CLS imaging.

Dye	Absorption (nm)		Emission (nm)		Stock Concentration	Working Solution	In Flow-cell
	DNA	RNA	DNA	RNA			
SYTO 9	485	486	498	501	3.34mM	2 μ L in 1mL dH ₂ O	1mL stain soln.

The dye was allowed a 30 min binding period by stopping the flow of synthetic feed and then a 30 minute washing period with synthetic feed to remove access stain. Images were captured using both the CLSM as well as epifluorescence microscopy.

2.5.2 Scanning Electron Microscopy (SEM)

A Hitachi S-3400N SEM with a variable pressure detector was used to acquire detailed images of the attachment substrate and bacterial growth in the flow-cell system. In order to construct a flow-cell from which samples could be extracted for SEM imaging, two

small pieces of glass slides were loosely attached to the bottom of the flow-cell chamber. The attachment substrate was then added, and the flow-cell was run for 8 days. At the end of the flow-system cycle, the flow-cell cover was removed and the loosely attached pieces of glass slide were ejected thus containing a sample meeting the dimension requirements for SEM. Using the loosely attached pieces of glass slide as bottom support, allowed for sampling of the attachment substrate with minimal disturbance to the surface matrix.

Before visualizing the sample using the variable pressure SEM, the sample was subject to a fixating agent solution (0.1M) composed of 4% paraformaldehyde and 1% glutaraldehyde, prepared in phosphate buffer at pH 7.5, which was used to insolubilize proteins by forming many cross-linkages with nitrogen groups in a short period of time helping the biomass withstand osmotic pressure from dehydration (Kiernan 2000); the solution was pumped directly into the flow-cell for a continuous 24 hours. Once the samples were removed from the flow-cell chamber, a series of alcohol dehydrations were performed in order to displace the water present in the attachment substrate. The samples were completely immersed in various concentrations of ethyl alcohol: 70%, 80%, 90% and 100%. For each successive dilution of alcohol, the samples were immersed for 30 minutes, with an additional 30 minutes for the 100% step to ensure thorough dehydration. The samples were then subject to critical point drying using liquid CO₂, which completely displaced the ethanol present in the attachment substrate. Finally, the samples were left in the 100°C oven over a period of 2 days to evaporate any remaining water fixed on the mounting stages for SEM and glued with colloidal graphite for stability and dispersion of charge from the electron beam. One coat of gold was added to each sample for increased conductivity, and the samples were then loaded in the SEM for visualization.

2.6 Molecular Analysis

2.6.1 Genomic DNA extraction

Total community DNA from microcosm was extracted from a batch culture using an UltraClean[®] Soil DNA isolation kit (Mo Bio Laboratories, Carlsbad, CA) following the manufacturer's protocol.

2.6.2 PCR amplification of 16S rRNA genes

PCR amplification of the 16S rRNA genes was performed using the bacteria-specific forward primer U341F (5'-CCTACGGGAGGCAGCAG-3') (Muyzer *et al.* 1993) and the reverse primer U758R (5'-CTACCAGGGTATCTAATCC-3') (Lee and Malone 1993). These primers, complementary to conserved regions of the 16S rRNA gene were used to amplify a 418-bp fragment corresponding to positions 341 to 758 in the *Escherichia coli* sequence and covered the variable regions V3 and V4. The bacteria-forward primer used for DGGE incorporated a GC clamp (5'GGCGGGGCGGGGGCACGGGGGGCGCGGCGGGCGGGGCGGGGG-3') at the 5' end. This GC-clamp stabilizes the melting behavior of the amplified fragments (Sheffield *et al.* 1989). Each 50 μ L PCR mixture contained \sim 1 ng/ μ L of the template DNA, 25 pmol of each oligonucleotide primer, 200 μ M of each dNTP, 2.5 units of Taq polymerase (New England BioLabs) and 1 x Taq polymerase buffer (10 mM Tris-HCl pH 9.0, 50 mM KCl, 1.5 mM MgCl₂). Briefly, after an initial temperature of 96°C for 5 min and thermocycling at 94°C for 1 min, the annealing temperature was set to 65°C for 1 min and decreased by 1°C every cycle for 10 cycles, with a 3 min elongation time at 72°C. Additional cycles (15-20) were performed with annealing temperatures at 55°C. PCR products were loaded onto a 1% agarose gel with SYBR Safe (Molecular Probes, Eugene, OR, USA), using a 100-bp ladder (New England BioLabs) to determine the presence, size and quantity of the PCR products.

2.6.3 Microcosm bacterial community Denaturing Gradient Gel Electrophoresis (DGGE) analysis

The 16S rRNA gene products from three PCR reactions were combined for each sample and concentrated by ethanol precipitation for DGGE analysis. About 450 ng of the 16S rRNA gene product was applied to a lane, and analyzed on 8% polyacrylamide gels containing gradients of 30-70% denaturant (a solution with 7M urea and 40% deionized formamide was considered to be 100% denaturant). DGGE was performed using a DCode Universal Mutation Detection System (Bio-Rad). Electrophoresis was run at a constant voltage of 80 V for 16 h at 60°C in 1x TAE running buffer. The gels were then stained with SYBRGold (Molecular Probes, Eugene, OR, USA), and imaged with the UVP BioDoc-It M26 imaging system. Individual bands from the DGGE gels were excised and eluted with 25 µL of dH₂O overnight at 4°C before being re-amplified with the same set of primers without the GC-clamp. One microliter of DNA was re-amplified with the appropriate corresponding bacterial or archaeal primers (without the GC clamp) as follows: an initial denaturation of 5 min at 96°C, followed by 30 cycles of 94°C for 1 min, 60°C for 30 sec, and 72°C for 1 min. PCR products for sequencing were purified using a Gel/PCR DNA Fragments Extraction Kit (IBI Scientific). Sequencing was performed at SickKids hospital with their respective primers. Raw sequence data were assembled in BioEdit v7.0 (Hall 1999). The sequences were manually aligned by comparing forward and reverse sequences. The occurrence of chimeric sequences was determined manually with the CHECK_CHIMERA function from the Ribosomal Database Project-II and Bellerophon.

CHAPTER 3: RESULTS AND DISCUSSION

3.1 Aerobic and anaerobic enrichments

The first step of the study was to enrich microorganisms of interest under both aerobic and anaerobic conditions. Under aerobic conditions, 0.2 g of tailings was added to 10 mL LB medium. At the end of the incubation period, substantial growth was determined as sediment in the 15mL falcon tubes, most forming white colored colonies when plated on LB agar. When the cultures were further transferred in anaerobic Fe(III) medium, no significant growth and no color change was determined in the medium suggesting whatever metabolic pathway might have been present was probably a form of fermentation rather than actual metal reduction. Fe(III) medium inoculated with tailings material showed significant metal reduction, observable by color change of the liquid from a dark red color to colorless liquid with black precipitate (Figure 3.1). The color change of the medium was caused by the production of FeO which is dark brown-black in color, while the colorless supernatant contained mostly dissolved Fe(II) ions (Yatsenko *et al.*, 2010, Roh *et al.*, 2007). The Fe(III) enrichments were performed under both near-neutral pH (7.5) and alkaline pH (9.5).

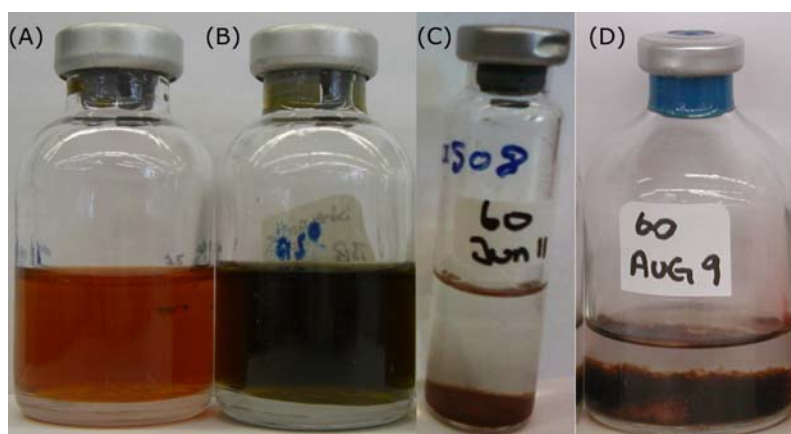


Figure 3.1. Anaerobic serum vials showing (A) color of sterile Fe(III) enrichment medium, (B) color change of Fe(III) medium inoculated with *S. putrefaciens* as a positive control, color change and precipitate of Fe(III) pH 7.5 medium (C) and pH 9.5 medium (D) inoculated with tailings material.

Cultures grown in an alkaline pH environment seemed to be more effective at reducing Fe(III), an observation based on rate of FeO precipitation and color change intensity. This suggested the possibility that at neutral pH, certain functional members of the consortium, that would normally be active at higher *in-situ* pH, are functioning at a lower rate and also that selection for alkalophilic bacteria occurred in the tailings. Clearly the preference for a high pH environment by the mixed community indicated that culture conditions, that may be optimum for well described laboratory strains but not formulated with a specific growth environment or metabolic function as criterion, are not necessarily best suited for the enrichment of functional communities from environments with distinctive characteristics. This result further suggests that these communities had been optimized for growth and proliferation under *in situ* conditions. The enrichment under aerobic conditions with subsequent transfer to Fe(III) anaerobic medium from LB aerobic medium showed that the members of the consortium responsible for Fe(III) reduction are not dominant under aerobic conditions, suggesting some members are anaerobic. The difference in color and state of the medium between the mixed community and the pure culture positive control *S. putrefaciens* could be explained by variations in metabolic pathways. In the flow-cell chamber during flow-system incubation, adsorption of the Fe(III) complex in the bacterial biofilm was seen, as well as the gradual change in color from the dark red to brown-black which signified presence of Fe(III) reduction, over the duration of the flow-system incubation period (Figure 3.2).

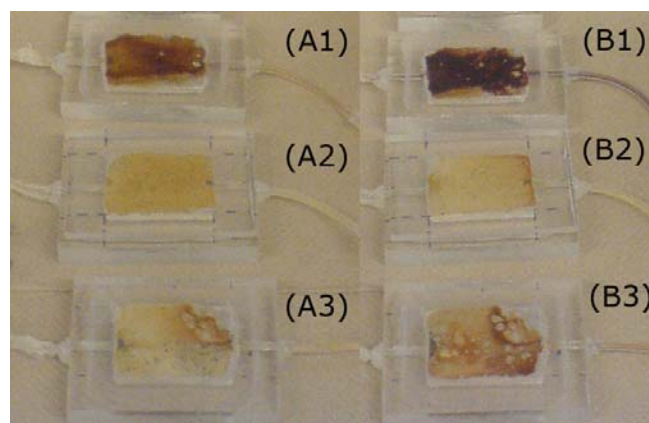


Figure 3.2. Visual determination of Fe(III) reduction and color change of synthetic feed of *S. putrefaciens*, sterile control and mixed community flow-cells after 1 day of incubation (A1, A2, A3 respectively) and after 3 days of incubation (B1, B2, B3 respectively).

The presence of abundant amounts of biomass in the form of flocs was not detected in any of the mixed community or pure culture *S. putrefaciens* vials, although slight turbidity was detected in the mixed community vials after the first few days of incubation. The lack of large amounts of biomass or flocs was to be expected, as Fe(III) reducing organisms very rarely present such growth characteristics. The use of labile or complex growth media could however, cause underestimation or exclusion of potential key members of the mixed community. All subsequent experiments were performed using enrichment sample #60 from core #20 (Appendix 1).

3.2 Redox Potential Measurements of Continuous Flow-Cell Systems

There is an inverse relationship between oxygen solubility in liquid and temperature, therefore purging the synthetic feed as soon as possible after removal from the autoclave enhanced the removal of O₂. Also, by continuously purging the synthetic feed while being cooled at room temperature, the diffusion of O₂ back in the liquid was restricted. Chemical agents for O₂ reduction, such as cysteine and sulfate salts were not used due to either possible decrease in pH values of the synthetic feed (in the case of cysteine), chemical reduction of Fe(III) by sulfate or the possibility of Fe(III) associated chelating agents precipitating at high temperatures in the presence of these chemical species. Once the synthetic feed was purged with N₂ gas, it was quickly placed in the airlock chamber of the anaerobic cabinet. Before starting the flow-cell system, the synthetic feed was allowed to acclimatize for 24 hours at the anaerobic chamber internal temperature of 25-27°C, with humidity levels ranging between 55-65%. Once the flow-cell system components were connected and the system started, before microbial inoculation, a redox potential reading was taken and recorded as time 0, indicative of the initial condition of the synthetic feed. Most values of Eh were recorded between ≥ 0 -120mV (Appendix 2), which is representative of an anaerobic environment as previously discussed in Chapter 1 and comparable with past flow-system experiments (Lim *et al.* 2008).

Figure 3.3 shows the change in Eh values recorded over an 8-day incubation period for positive control pure culture *S. putrefaciens*, mixed community and sterile negative control. The first 24 hours of incubation in the flow-system showed a significant decrease in

Eh of 150mV for the mixed community and 330mV for positive control. This can be explained as rapid metabolic activity required for adaptation to the new environment. As opposed to enrichment batch cultures, the flow-system is a significantly different environment, where microbial cells are subject to shear forces by the flow-rate across the substrate attachment surface as well as constant supply of nutrients, compared to a finite initial nutrient supply in the case of batch culture.

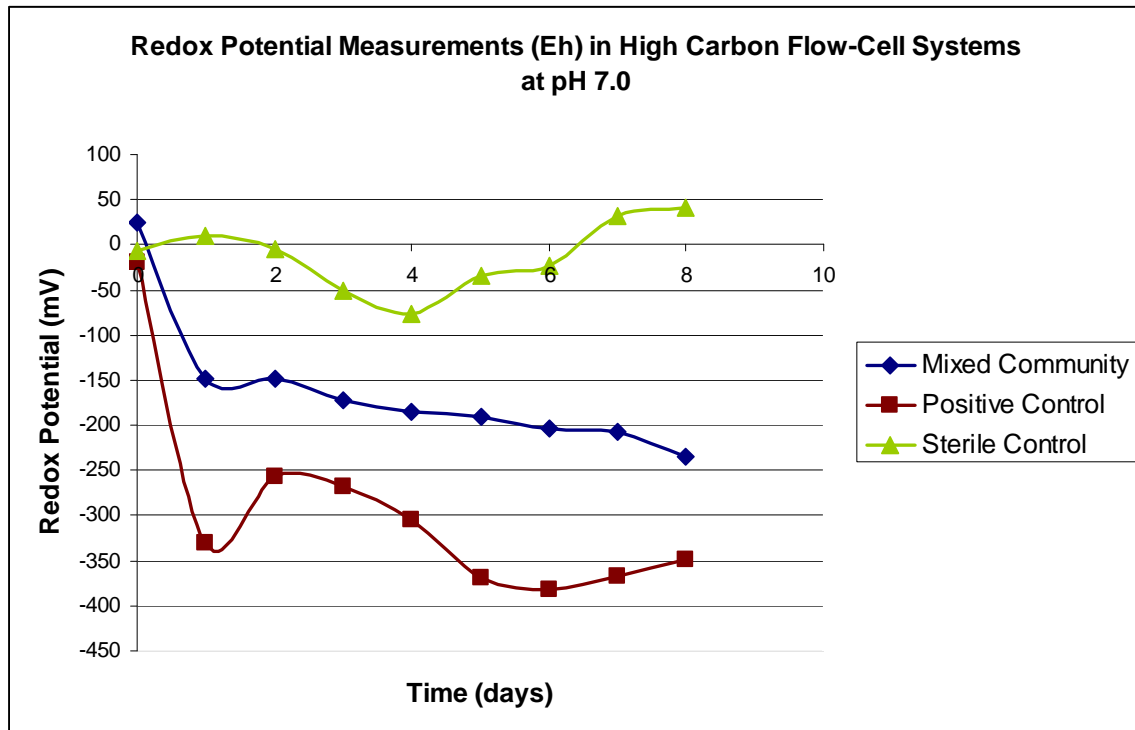


Figure 3.3. Graphical representation of the change in Eh in flow-cell systems over an 8 day incubation period under high carbon (0.9 g/L lactate and citrate) neutral pH conditions.

The Eh presented with an overall decrease by the end of the incubation period, from -20.2mV to -382.5mV in the positive control (Appendix 2), suggesting constant metabolic activity. However, the profile shows a rather unusual Eh value at day 1, which does not fit the rest of the Eh profile, suggesting this reading may be an outlier. Omitting the Eh reading at day 1 would make this profile look much more as expected. The lowest Eh values were recorded after an incubation of 5 days for the positive control, suggesting that at this point, this organism had reached optimum growing conditions. These values are comparable with past experiments done on *S. putrefaciens* in flow-system with high nutrient conditions (Lim

et al. 2008; Masscheleyn 1991). The mixed community showed a slower metabolic activity, with Eh decrease from 25mV to -234.9mV (Appendix 2); however, this was to be expected considering that the environment this consortium was isolated from is characterized as extreme, in terms of organic carbon (20 mg/L), pH (9-10) and temperature (4-6°C). The hypothesis is that the investigated metabolic activities are performed by a microbial consortium rather than a single individual organism, in which case it is possible that the metabolites of one organism will supply requirements for the next. This increased the chance that certain metabolic pathways of the consortium members have differences in reaction rates. Together with probable differences in optimum growth temperature of the test strain (positive control, 25-30°C) (Bowman *et al.* 1997) and the *in situ* community, this model could explain the significant differences between the mixed community and pure culture positive control. The Eh readings also showed sustained metabolic activity for the mixed community although it appeared that a steady state was not reached during the incubation period. The Eh profile of the mixed community also showed an overall decrease in Eh values by the end of the 8-day incubation period. It is possible that comparable Eh values between mixed community and pure culture could have been recorded if the mixed community incubation time would have been increased. The Eh readings for the sterile control had some variation between days 3 to 5 which could be explained by changes in gas concentrations in the anaerobic chamber due to regular flushing to maintain steady H₂ levels (2-3%) as well as consistent usage of the airlock chamber. According to the Coy Laboratories instructions manual, regardless of how many times the airlock is cycled there will always be a small amount of oxygen entering the chamber, found to enter across the chamber floor (Coy Laboratories Inc.). The ambient O₂ concentration of 209,000 ppm will get diluted to approximately 7,639 ppm in the airlock chamber after 3 cycles of vacuum at 24inch mercury, 2 cycles of N₂ flushing and 1 cycle of gas mixture flushing (Coy Laboratories Inc.). This concentration will be diluted in the much larger volume of the anaerobic chamber to approximately 200 ppm O₂, which should be easily reduced by the hydrogen present as well as the palladium plate catalysts. This reaction however is not instantaneous, and small amounts of oxygen could be introduced to the flow-system over the peristaltic pump, a phenomenon which could explain the slight variations in Eh values. Slight temperature

change inside the anaerobic chamber could also affect the solubility of the residual O₂ as well as other gases in the synthetic feed which subsequently causes Eh readings variation. Nonetheless, the sterile control experiments show no evidence of abiotic decrease in Eh due to chemical factors other than microbial activity, values which are stable in a range of 41.0mV to -76.40mv.

Following flow-cell experiments with a high carbon content synthetic feed, the mixed community and pure culture *S. putrefaciens* were exposed to a low carbon content environment (20 mg/L lactate and citrate), at alkaline pH (9.5), comparable to the conditions in the DTMF. Figure 3.4 shows the redox profile that evolved due to microbial metabolic activity in this oligotrophic alkaline pH environment.

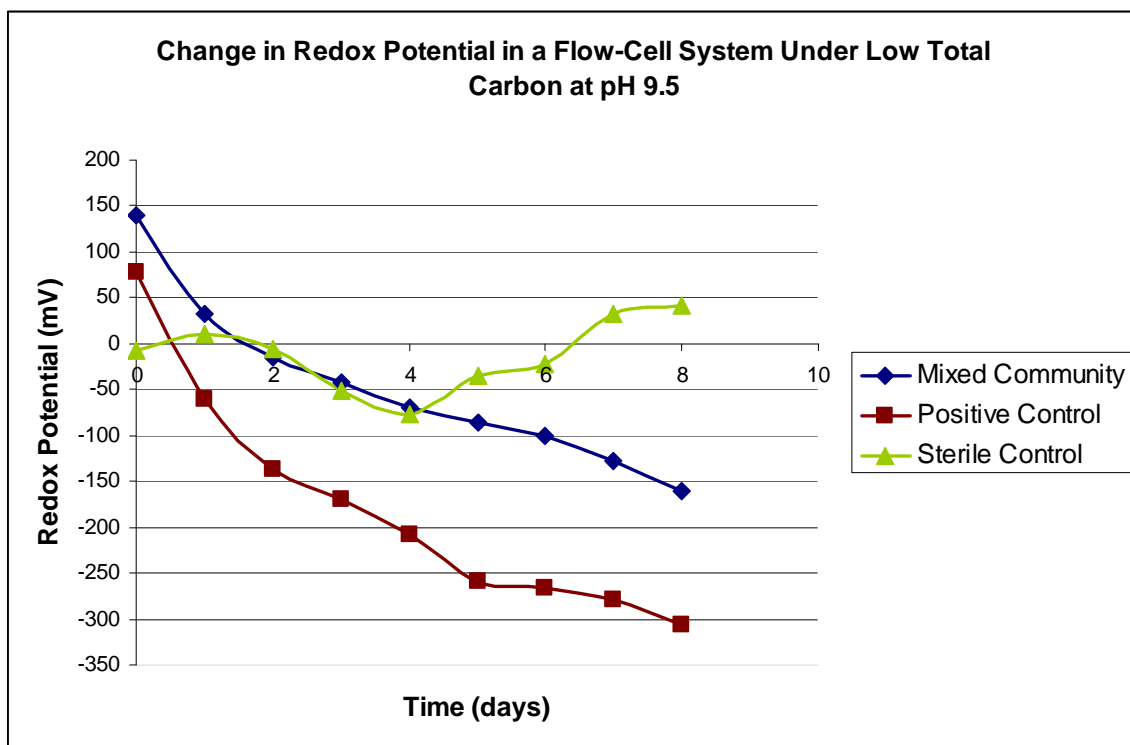


Figure 3.4. Graphical representation of the change in Eh in flow-cell systems over an 8 day incubation period under low carbon (20 mg/L lactate and citrate), alkaline conditions.

As expected, the change in organic carbon concentration from 0.9 g/L lactate/citrate to 20 mg/L lactate/citrate caused a significantly slower metabolic rate for both mixed

community and positive control as measured by the Eh profile. The first observation made was that compared to metabolic activity under a high carbon environment, the first 24 hours of the incubation time no longer presented with a significant decrease in Eh. The mixed community was unable to decrease the Eh below 0mV (31.7mV, Appendix 2) in the first 24 hours of cultivation on low carbon conditions, as opposed to previous high carbon experiments in which the Eh after 24 hours was measured at -148.2mV. A similar difference in Eh values can be observed for the pure culture positive control, for which the Eh was recorded at -60.2mV after 24 hours as opposed to -329.8mV. As Figure 3.4 shows, the rate of Eh decrease of the positive control was faster; however, in neither of the cases was a steady state reached over the 8-day incubation period. Although the organic carbon content was equivalent to DTMF *in situ* conditions, the incubation time of the flow-cell system is very short compared to the retention time of the tailings in the storage pond. The incubation temperature of the flow-cell system (25°C) is also un-representative of the DTMF conditions (4-6°C), and this would be a logical control that remains to be examined. The mixed community microorganisms however did show the capability of changing the Eh well below 0mV, conditions under which heavy metals can be solubilized. It should be noted that in these experiments the flow-system provided a constant supply of carbon, which is in contrast to the TMF, where slow (diffusion dominated) flow rates in the tailings body means the finite pool of carbon present will be rapidly depleted.

3.3 Ferrous Iron Production in Continuous Flow-Cell Systems

In order to determine the potential degree of microbial Fe(III) reduction, the ferrozine colorimetric method was used (Viollier *et al.*, 2000). The ferrozine reagent (monosodium salt hydrate of 3-(2-pyridyl)-5,6-diphenyl-1,2,4-triazine-p,p'-disulfonic acid) proposed by Stookey (1970), reacts with divalent Fe to form a stable magenta complex (Viollier *et al.*, 2000). Figure 3.5 shows Fe(II) concentrations produced via microbial Fe(III) reduction under high carbon conditions. The positive control (*S. putrefaciens*) reduced ferric iron within the first 24 hours of incubation, which correlates with the sharp decrease in Eh, shown earlier, during this time frame. Metabolic activity appeared to have remained constant throughout the 8 day incubation period, as suggested by the consistent Fe(II) concentrations around

200 mg/L (Appendix 3). This trend showed the positive control quickly reached stable growth. The constant rate of 200 mg/L Fe(II) further suggests the capability of Fe(III) reduction by *S. putrefaciens* is not only limited to soluble chelated forms of iron (94.95 mg/L in synthetic feed), but also capable of reducing crystalline forms of Fe(III), a component of the kaolin clay-sand mixture of unknown concentration (Bristow *et al.* 2002; Rhodes 2000), which was used as the attachment substrate in this study.

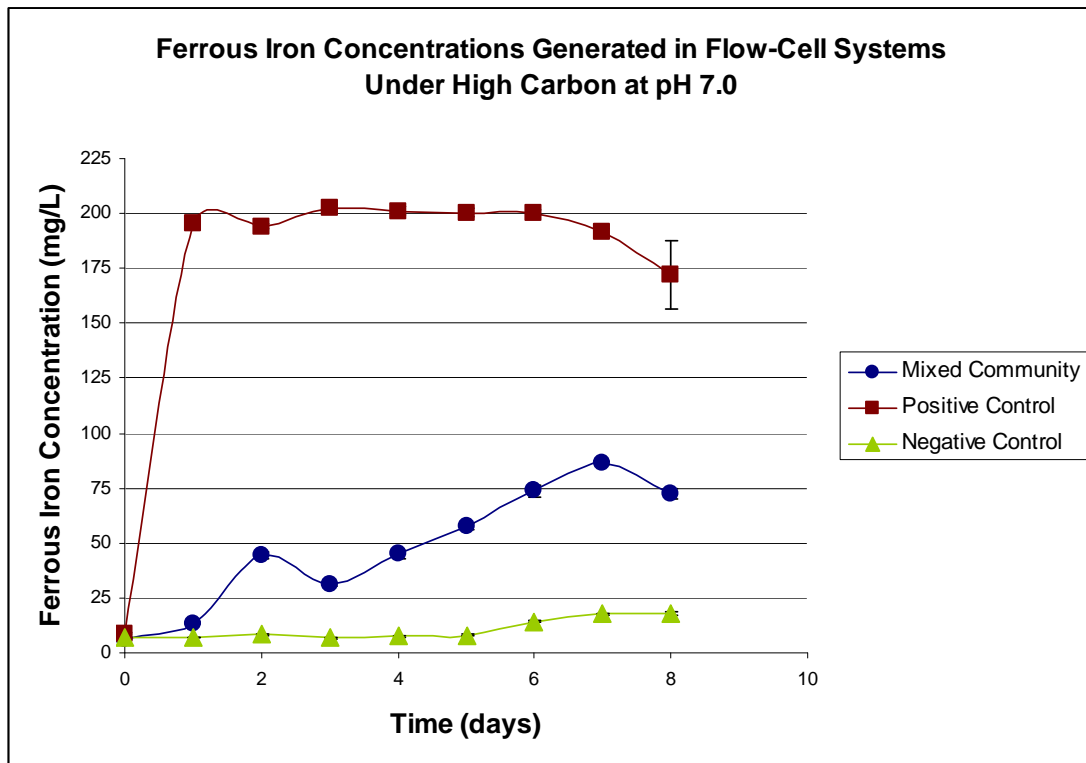


Figure 3.5. Ferrous iron concentrations recorded in flow-cell systems under high carbon conditions at neutral pH.

S. putrefaciens proved to be very effective at reducing Fe(III) under low flow-rate conditions (16.6 cm/hr at the clay-liquid interface) with a hydraulic retention time (HRT) of 16.2 min (0.27 hrs) for the synthetic feed inside the flow-cell chamber. These physical parameters of the synthetic feed in the flow-cell chamber allowed the organisms enough time to reduce all of the more bioavailable soluble Fe(III) from the synthetic feed while still reducing some of the crystalline Fe(III). Based on Fe(II) concentrations measured from the flow-cell inoculated with the mixed community, it is clear that under high carbon conditions, the community is

capable of Fe(III) reduction. Considering the slow activity of the mixed community, and the incubation time required for batch enrichments, it is safe to assume that the mixed community will most likely begin reducing the soluble and more bioavailable form of Fe(III) before beginning to reduce other crystalline sources of Fe(III). This is evident from the highest measured Fe(II) concentration of 92.37 mg/L (Appendix 3), which would represent most of the Fe provided in the trivalent form from the synthetic feed. Since the Eh profile for mixed community metabolic rate indicates a much slower activity than measured in the positive control, increasing the incubation time of flow-cells under high carbon conditions will most likely result in a similar trend with the one observed in the positive control. The flow-system experiments were meant to provide a baseline for future studies of lower flow-rate environments, which will be more representative of *in situ* conditions.

Figure 3.6 shows Fe(II) production via microbial metal reduction under low carbon conditions. The negative control experiment does show a very low concentration of Fe(II), which is to be expected as background levels due to chemical equilibrium between the Fe(III) and Fe(II) species in the synthetic feed.

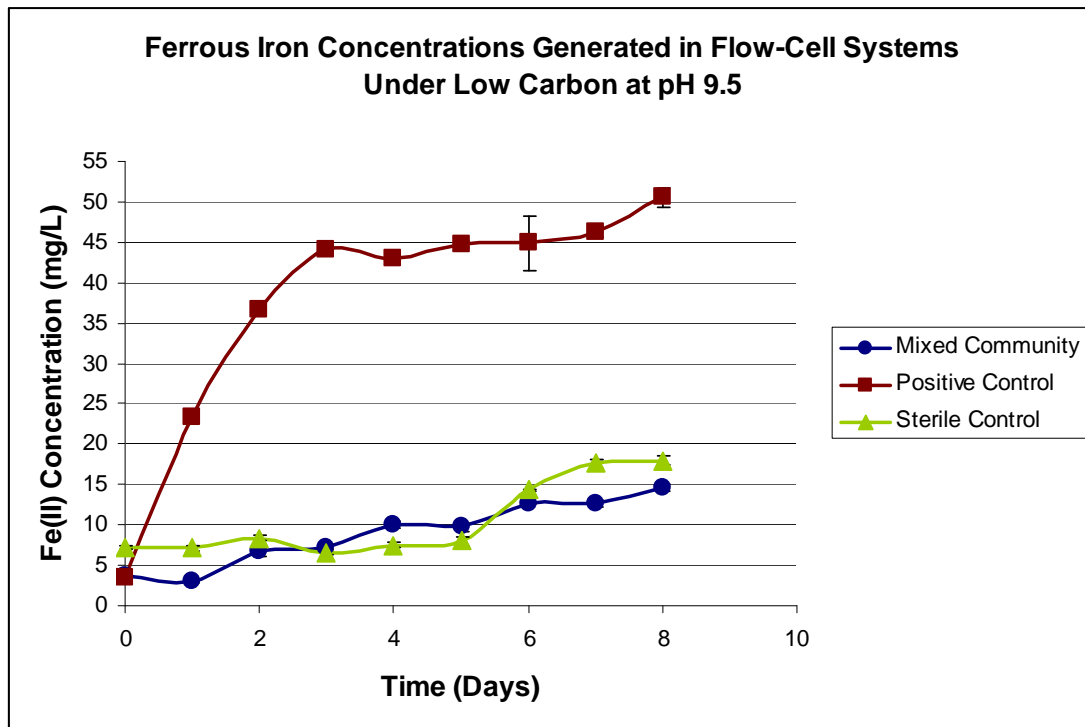


Figure 3.6. Ferrous iron concentrations recorded in flow-cell systems under low carbon conditions at alkaline pH.

There is however a slight deviation from the first 5 days concentrations of 6-8 .mg/L Fe (II); this could be due to variations in Eh values which affected the Fe(III) speciation on a very small scale. The negative control experiment also could have been affected by unnoticed contamination, either in the flow-cell chamber itself or at the OR probe port. As expected, subjecting the microorganisms to a low organic carbon environment caused a significant decrease in metabolic rate. At a first glance, the mixed microbial community Fe(II) production seemed to be insignificant compared to the negative control experiment, particularly due to the above mentioned variation in the last three values. However, analyzing the data (Figure 3.7) revealed a pattern characterized by a slow and steady increase in Fe(II) concentration values every 48 hours rather than a gradual increase between consecutive sampling times.

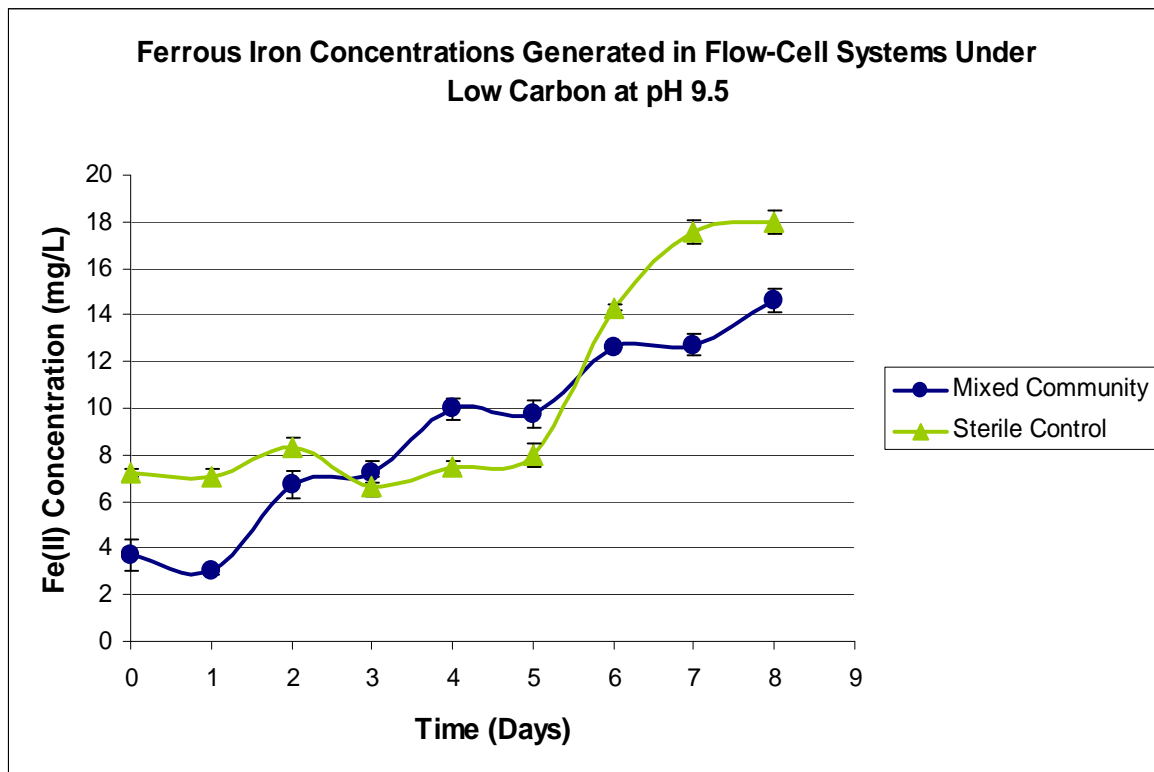


Figure 3.7. A closer look at the relationship between Fe(II) concentration values in a mixed community flow-cell over the duration of low carbon incubation.

The largest Fe(II) concentration detected at the end of the 8 day incubation period was 14.62 mg/L (Appendix 3), although increasing the incubation period will most likely provide a better understanding of microbial activity, a modification which could prove beneficial due to the generally slower metabolic rates of the isolated mixed community, but relevant in terms of microbial activity in the DTMF sediment. At such a low rate of Fe(III) reduction, it is assumed that the soluble form of Fe(III) in the synthetic feed is the final electron acceptor used since it would be thermodynamically more favorable for the cells to use nutrients that are more readily available, rather than crystalline sources of Fe(III). It is possible that, under *in situ* oligotrophic conditions, the members of the mixed microbial community are capable of surviving with metabolic activities that are insignificant on the bulk integrity of the DTMF on a short term scale however prove to be relevant for long-term predictions. The positive control metabolic rates were also significantly impacted by the decrease in organic carbon content, with the maximum Fe(II) concentration being recorded at 50.61 mg/L (Appendix 3), compared to previous high carbon flow-cell Fe(II) concentration of 200 mg/L. Clearly microbial Fe(III) reduction is linked to available organic carbon content, a condition not only true for the mixed microbial community but for pure culture as well. As mentioned in Chapter 1 *S. putrefaciens* has a pH growing optimum of 6-9, and the mixed microbial community presented with a more effective metabolic activity under high pH enrichments. Thus carbon acquisition seems to be the rate limiting step in the metabolic pathway for the organisms tested, rather than pH range.

3.4 Microscopy of Attachment Substrate: Confocal Laser Scanning and Scanning Electron Microscopy

In order to determine if the metabolic activity of the mixed community isolated from the DTMF tailings can be related to growth patterns and biofilm formation, microscopy was performed on the attachment substrate. Confocal laser scanning microscopy (CLSM) was used for its efficiency of distinguishing microbial cells, tagged with the SYTO®-9 nucleic acid probe, from the elaborate matrix of the clay and sand mixture. Epifluorescence microscopy imaging was also used, as this approach provided additional 3-dimensional details about the interaction between the microbial cells and the attachment substrate.

Scanning Electron Microscopy (SEM) was used to acquire more detailed images of possible EPS production by microbial cells during biofilm formation on the attachment substrate as well as any other physical relationship between bacterial cells in the biofilm matrix. Both imaging methods were used on flow-cells inoculated under high and low organic carbon to determine how carbon availability impacts biofilm development and microbial growth patterns on the attachment substrate.

CLSM images of the flow-cells under high carbon conditions revealed the mixed communities' ability to form copious amounts of biomass at the clay-liquid interface (Figure 3.8), as well as determining cellular orientation at the clay-water interface.

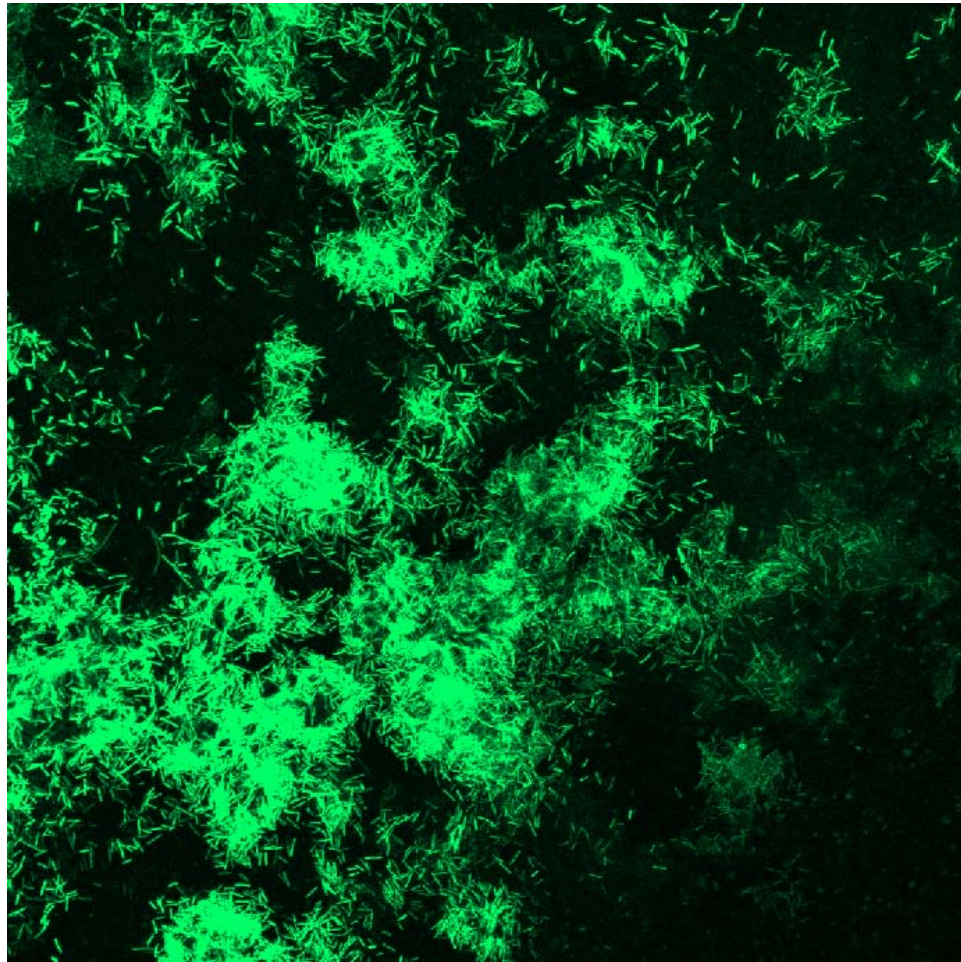


Figure 3.8. An *in-situ* CLSM image (60X-oil immersion) of a high carbon flow-cell chamber showing considerable amounts of biomass at the clay-liquid interface, after an 8-day incubation period suggesting biofilm formation.

All the CLSM images were taken using the 60X oil immersion objective with a 0.13 mm focal length. As mentioned in Chapter 1, the proximity between microbial cells and the final electron acceptor is very important in bacterially mediated redox reactions. The large amount of biomass that can be seen in Figure 3.8 could be explained by biofilm development on the attachment substrate. The bacterial cells seemed to have colonized the clay surface in layers of cells rather than individual small cellular aggregates suggesting production of EPS. A better three dimensional representation of the relationship between the biofilm produced and the attachment substrate can be seen in Figure 3.9, acquired using epifluorescence microscopy with the same objective, on the same flow-cell. This image shows the unique topography of the attachment substrate densely covered by the bacterially produced biomass.

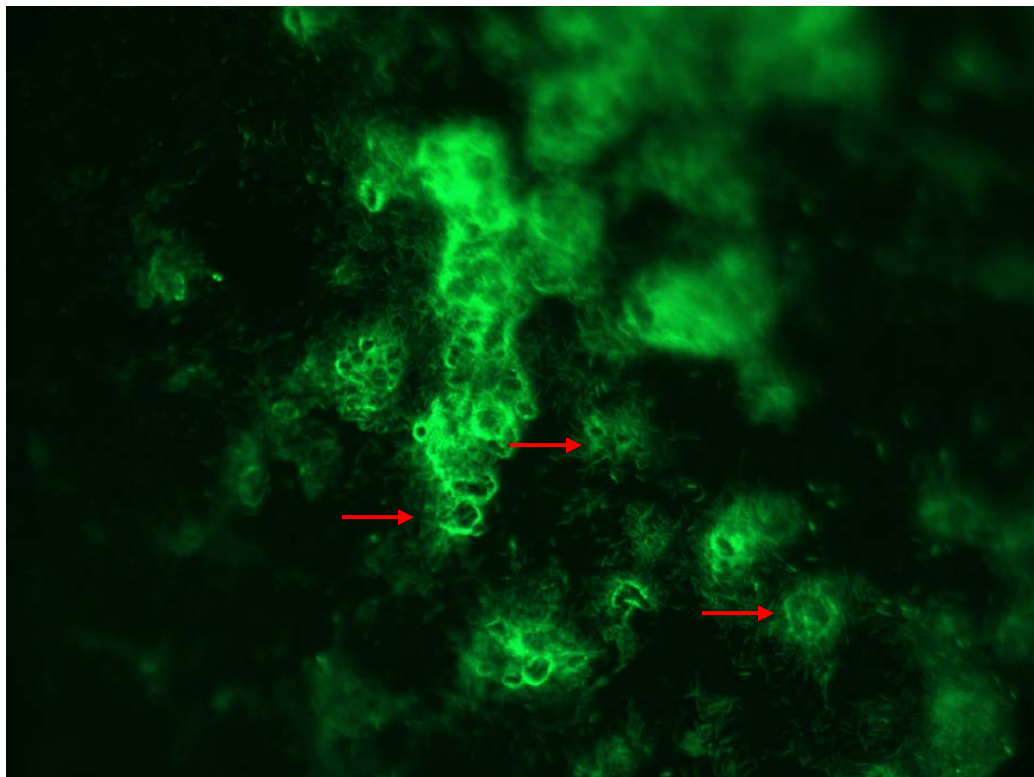


Figure 3.9. An *in-situ* epifluorescence microscopy image (60X–oil immersion) of a high carbon flow-cell chamber, at neutral pH; arrows show biomass production by microbial cells and colonization of the clay-sand substrate.

It is evident from these images, that the mixed microbial community formed strong interactions with the attachment substrate and was capable of producing large quantities of biomass under high carbon conditions. The attachment to the clay-sand substrate rather than

flocculent or planktonic growth suggested that the aluminum silica in the kaolin clay allowed adsorption of the Fe(III) complex therefore increased the proximity between Fe(III) and cellular outer membrane which helped facilitate microbial Fe(III) reduction. It is also possible that the amount of EPS produced by the cells was abundant enough to capture sufficient amounts of the Fe(III) soluble complex, causing the bacterial cells to colonize the attachment substrate. The growth pattern seemed to be consistent with areas inside the flow-cell that experienced higher concentrations of nutrients, notably at the inflow port. Although the volume of the mixed community inoculated into the flow-cell chamber was sufficient to cover the entire surface of the attachment substrate, most of the growth was observed close to the inflow port. This could be an indirect effect of the low flow rate (16.6 cm/hr) and, potentially, preferential flow channels inside the flow-cell chamber. As the synthetic feed flowed into the chamber, organisms situated at the inflow port acquired a large portion of the carbon source, thus reducing the amount of carbon reaching the outflow region of the flow-cell.

In order to determine biofilm and EPS production by the mixed microbial community, SEM was used on sections of the attachment substrate that were removed from the flow-cell chamber.

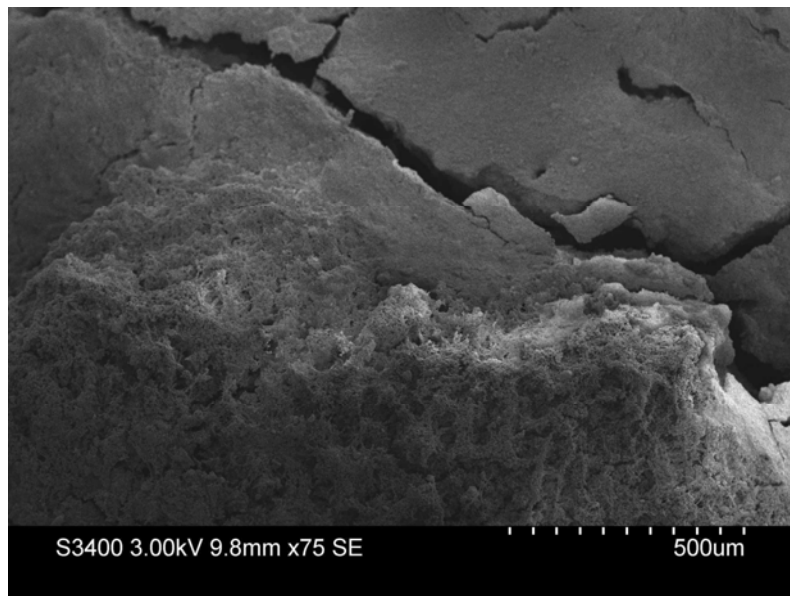


Figure 3.10. SEM image of biofilm formation by the mixed community on the surface of the attachment substrate under high carbon conditions at neutral pH.

Under high carbon conditions, the mixed community produced large quantities of EPS, forming an elaborate matrix on the surface of the clay substrate. Figure 3.10 shows the biofilm matrix produced on the attachment substrate as a network of EPS. The biofilm matrix can be seen on the bottom portion of the micrograph as a layer of biomass covering the attachment substrate, while the upper portion of the micrograph shows the texture of the clay substrate. This type of imaging was useful in differentiating between biomass covered areas of the attachment substrate and areas of the clay-sand material that did not present with significant biofilm formation. The high carbon environment prompted the microorganisms to produce enough EPS to cover large areas of the substrate which probably traps nutrients from the synthetic feed as well as causing sorption of inorganic ions such as Fe(III). Therefore the EPS not only acted as a connective network between bacterial cells, but also provided an adequate environment for Fe(III) reduction by connecting cells and final electron acceptor. SEM images also revealed an interesting network of EPS fibers connecting bacterial cells, as seen in Figure 3.11.

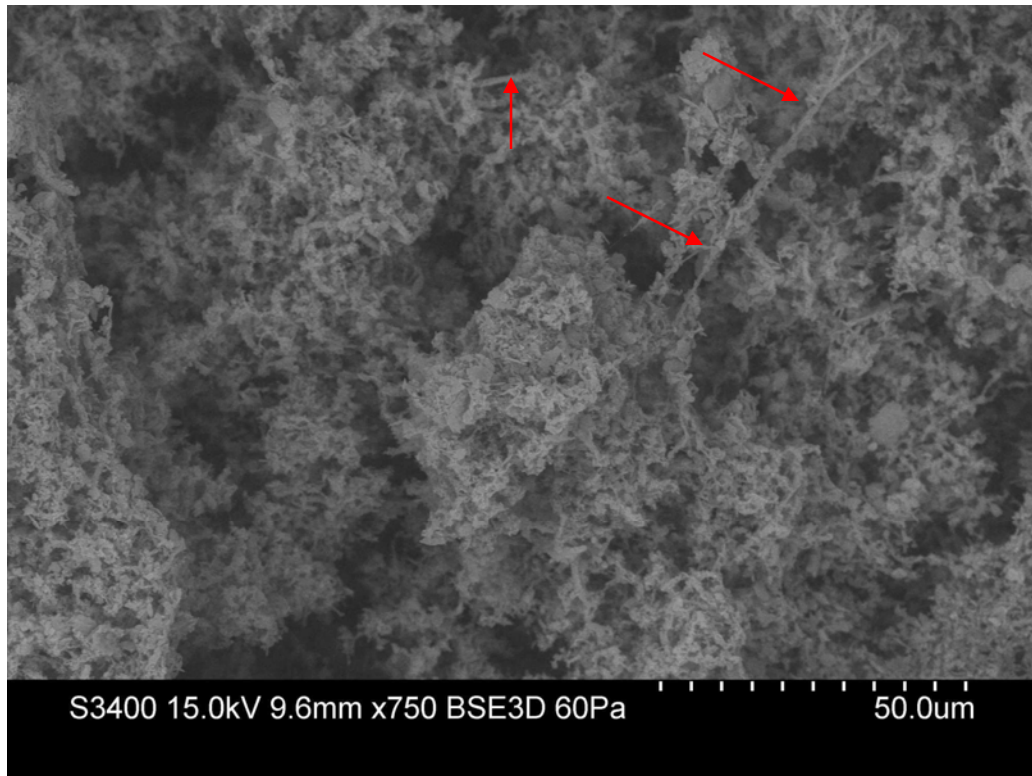


Figure 3.11. SEM image showing EPS connecting strands in the biofilm network under high carbon conditions at neutral pH.

These connections formed between various regions of the biofilm and between microbial cells (shown in Figure 3.12 and 3.13) could have played an important role in the successful function of the individual metabolic pathways of the community members as a single process. These networks could prove important in situations where byproducts of one organism provide nutritional requirements for another.

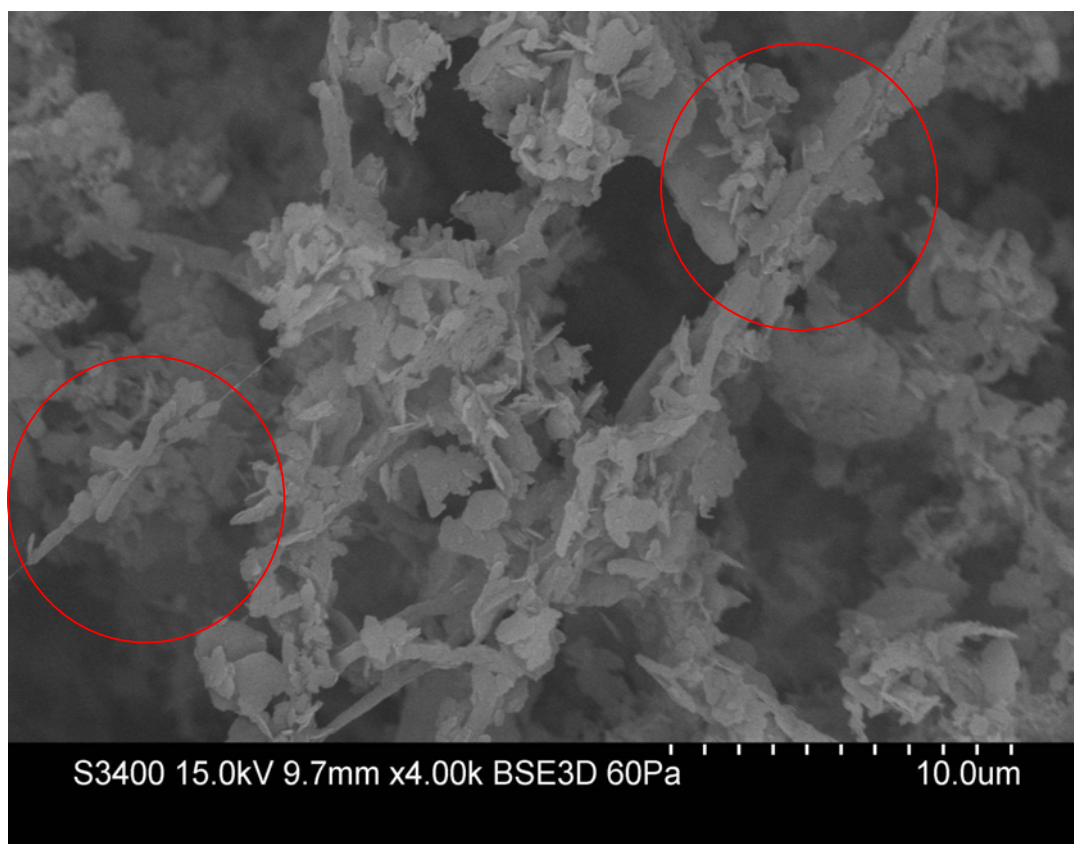


Figure 3.12. SEM image showing the connecting relationship between bacterial cells and the EPS strand network under high carbon conditions at neutral pH.

The production of a biofilm network by the mixed community seemed not only to provide a sources of nutrients and ease of access to a final electron acceptor but also aggregation of bacterial cells which essentially enabled bridging between cells, temporary immobilization of bacteria on the attachment surface, development of high cell densities and cell-cell recognition (Flemming *et al.*, 2010). In a flow-system environment where nutrients are continuously available, as opposed to a batch culture, it is beneficial that the cells colonize,

be immobilized on the surface and establish an efficient consortium from a metabolic pathway objective.

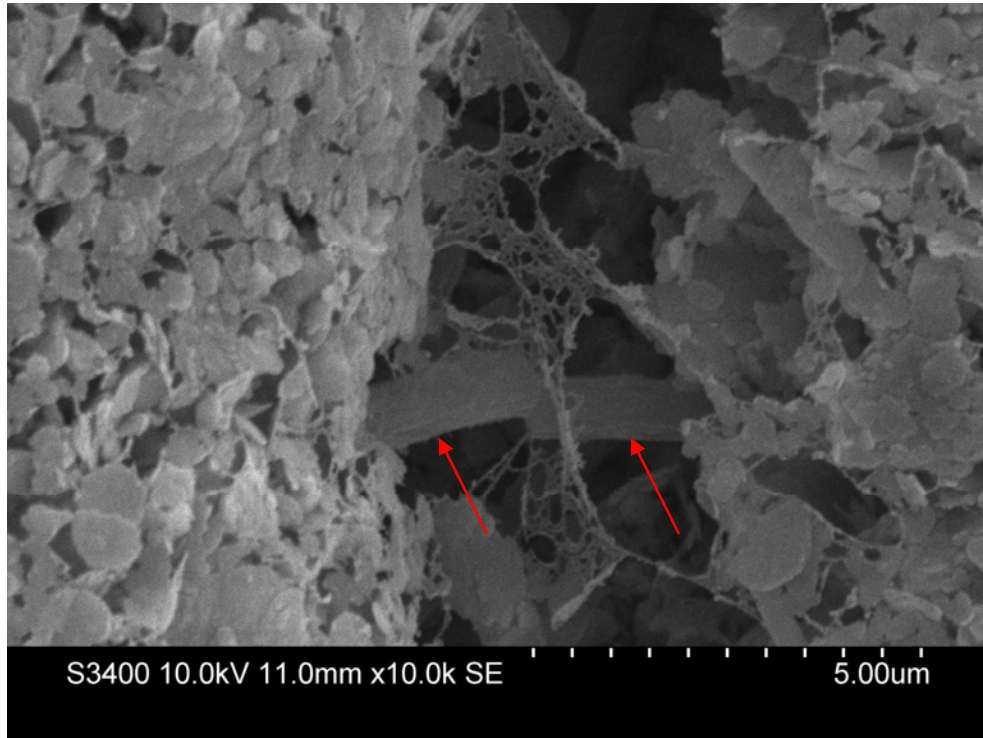


Figure 3.13. SEM image showing close interaction between microbial cells (red arrows) and production of EPS connecting network in a micro-environment on the attachment substrate, under high carbon neutral pH conditions.

Although under high carbon conditions the production of biofilm and EPS is evident with copious amounts of biomass produced, microbial growth patterns were significantly altered when exposed to a low carbon environment. Epifluorescence microscopy images (Figures 3.14 and 3.15) show that in low carbon flow-cells, the amount of biomass on the attachment substrate was very limited. Moreover, bacterial growth was seen as cell aggregates rather than a well established layer, suggesting carbon deprivation had significantly decreased microbial capability of biofilm formation. The cells were also significantly smaller compared to images taken under a high carbon environment, suggesting microbial metabolic rates may have drastically reduced to cope with the oligotrophic environment. After 24 hours of incubation, the flow of synthetic feed across the attachment substrate surface was no longer uniform but rather preferential, through small channels created by the liquid. The distance

between microbial cells and the 60X objective could have been significantly increased due to bacterial growth being limited to areas of high nutrient flow. Substrate areas that did not experience the same flow rates but were closer to the objective's focal length distance did not present with bacterial growth because of very low carbon and nutrient concentrations.

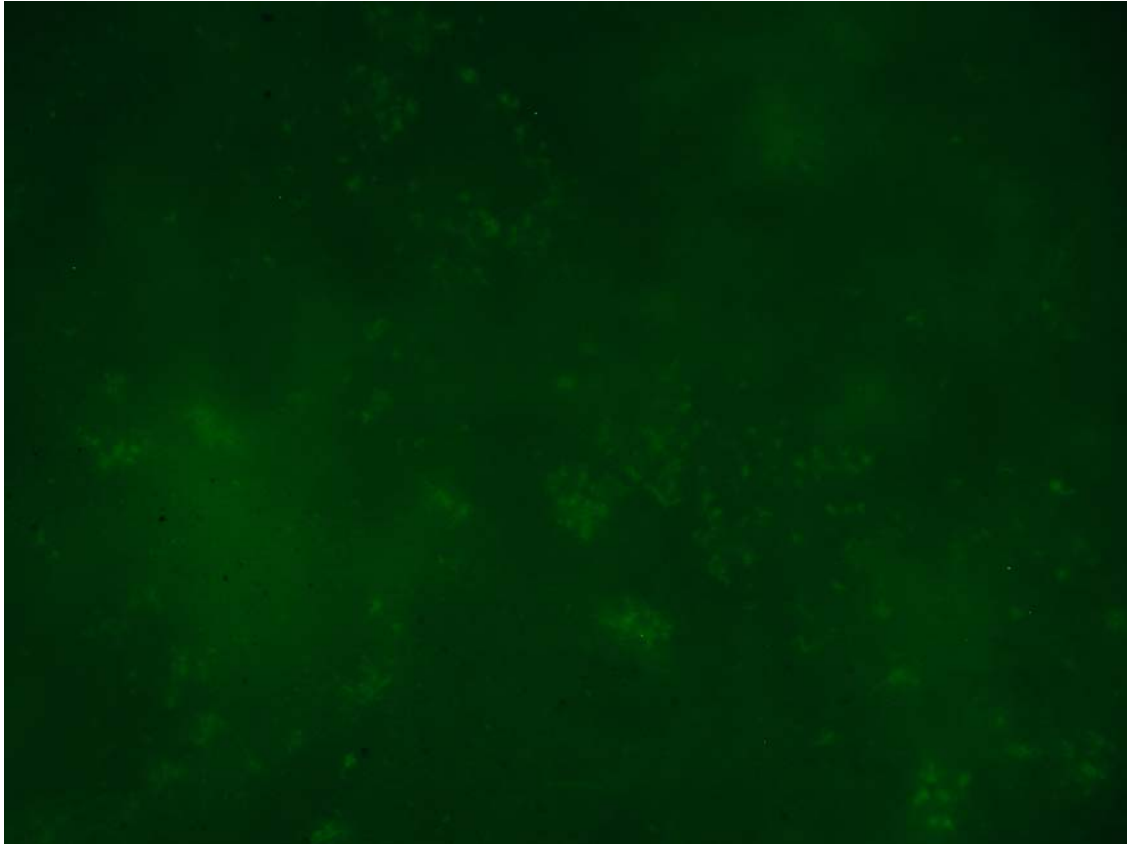


Figure 3.14. Epifluorescence microscopy image (60X-oil immersion) of a low carbon flow-cell chamber showing limited microbial growth on the attachment substrate and significant decrease in microbial cellular size, pH 9.5.

The significant decrease in surface area colonized and biofilm production by the mixed community could explain the decrease in Fe(III) reduction discussed in section 3.3. If the members of the mixed microbial community function in a symbiotic relationship of Fe(III) reduction, than the increased distance between bacterial cells and the lack of cellular interaction and communication could have also slowed down the metabolic rate. Reduced levels of EPS production and biofilm formation deprived the cells of a sink for excess energy and the sorption of inorganic ions was reduced.

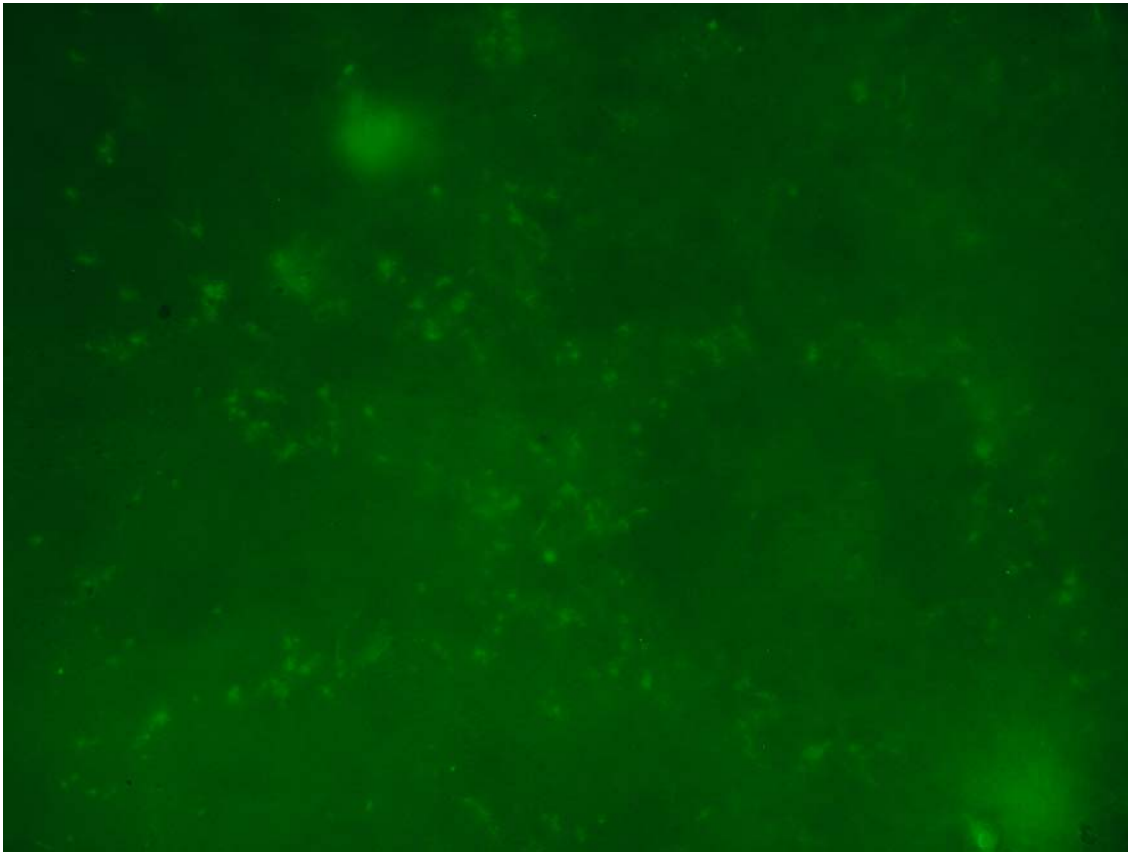


Figure 3.15. Epifluorescence microscopy image (60X-oil immersion) of a low carbon flow-cell chamber showing random growth of bacterial cells in small aggregates, pH 9.5.

SEM images of the extracted attachment substrate (Figures 3.16 and 3.17) from low carbon flow-cells have also revealed the complete absence of biofilm formation. Bacterial cells were difficult to visualize, possibly due to washing caused by loose adherence to the clay-sand substrate. Under high carbon conditions, the large production of EPS could have provided structural support for the clay material itself when removed from the flow-cell chamber for SEM sample preparation. Switching the synthetic feed to fixing agent in order to treat samples for SEM, could have washed away bacterial cells from the attachment substrate due to exposure to an already carbon deprived environment. Under high carbon conditions, the presence of large quantities of EPS would have secured the cells on the attachment substrate, which allowed for easy characterization of bacterial growth. SEM imaging for flow-cells incubated under low carbon conditions did not prove to be suitable due to requirements of sample preparation which disrupted the flow-cell chamber environment.

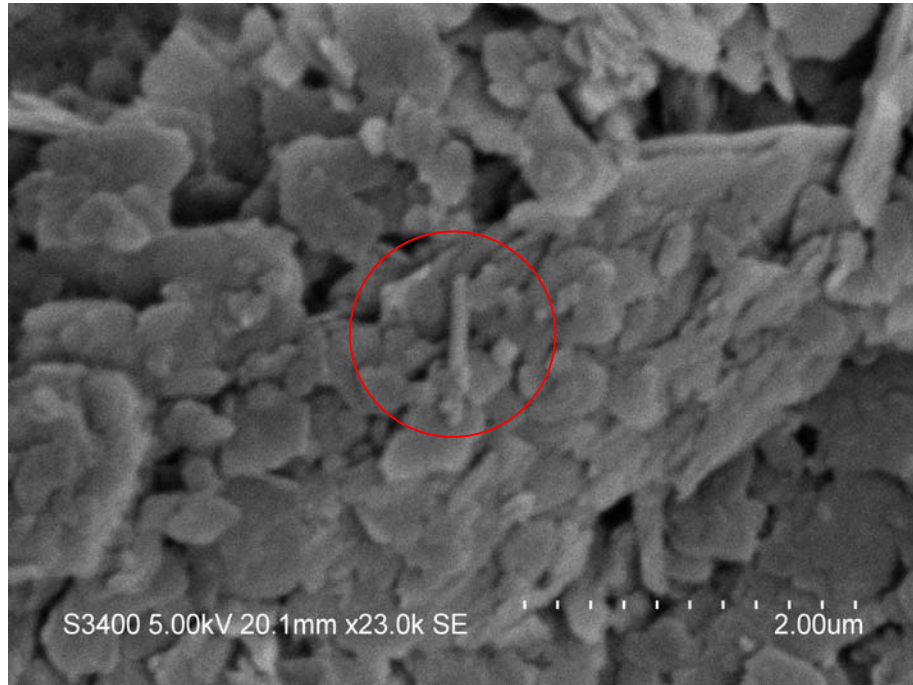


Figure 3.16. SEM image showing a single bacterial cell rather than biofilm formation on attachment substrate material, an effect of carbon deprivation.

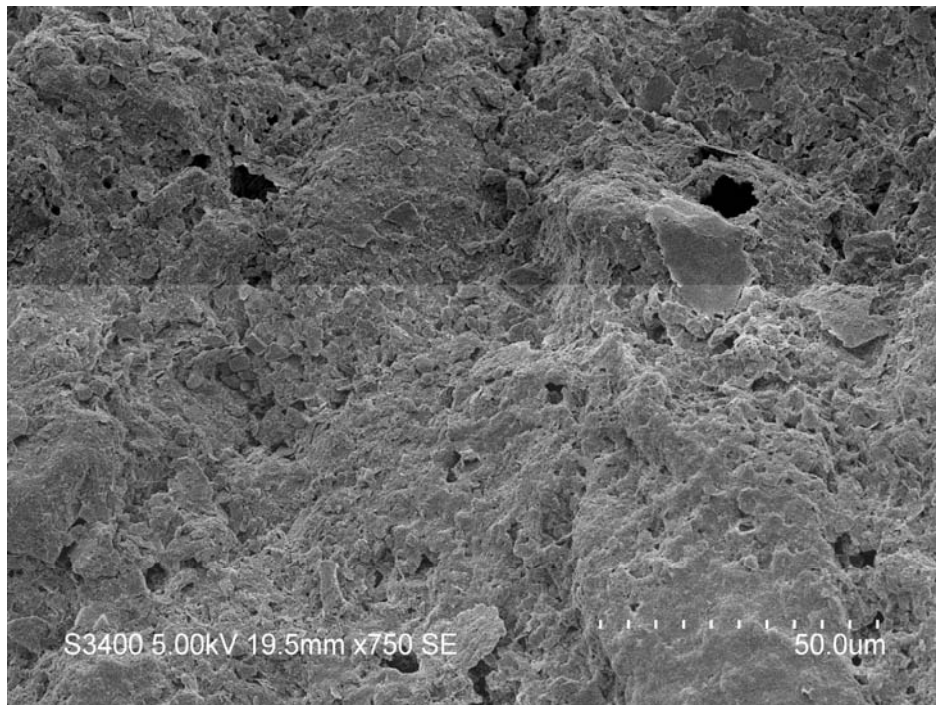


Figure 3.17. SEM image showing absence of biofilm formation and channeling created by preferential flow of synthetic feed on the attachment substrate under low carbon conditions, at pH 9.5.

3.5 Molecular Work and Identification of Mixed Community Members

To gain a better understanding of the Fe(III) redox reactions due to microbial metabolic activity, the mixed community DNA extracted from batch enrichments was subject to DGGE for band separation and sequenced for identification of the members of the consortium. The DGGE revealed the mixed community responsible for Fe(III) reduction in batch and continuous systems was composed of at least three different organisms.

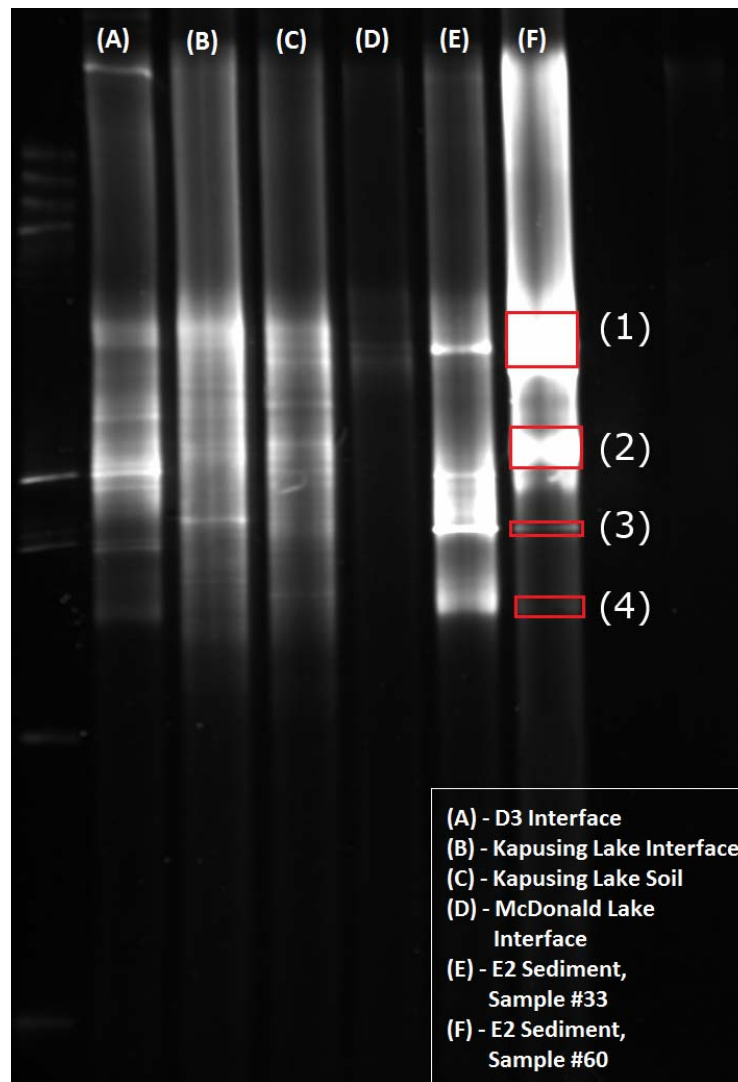


Figure 3.18. DGGE image showing 4 distinct bands for enrichment sample #60 used in this study, against other samples enriched under similar conditions.

Sequencing of DGGE bands determined these organisms belonging to species of *Pseudomonas* (bands 1 and 2), *Clostridium* (band 3) and *Rhodococcus* (band 4) (Figure 3.18). The DGGE profile for this mixed community showed four distinct bands (Figure 3.18) indicating four different Fe(III) reducing organisms; however DNA in bands 1 and 2 could actually originate from the same organism based on the sequencing results (Table 3.1). It is possible that several other species of microorganisms were present in the Fe(III) reducing community, but their DNA sequences not amplified due to lower number of 16S genes or extraction problems. It is unclear which of the members sequenced were dominant in the community since DGGE is not a quantitative method, and band intensity is most likely a representation of the abundance of amplified DNA sequences rather than microorganism numerical dominance. The *Pseudomonas* spp. are considered to be r-strategist organisms, which means these species can respond with large population increases when the opportunities become favorable (De Leij *et al*, 1995). R-strategists have poor competitive abilities, lack long term survival mechanisms and their numbers generally decrease rapidly once the favorable environment changes (De Leij *et al*, 1995). In the mixed community, the presence of potentially two species of *Pseudomonas* could be explained as a response to the increased carbon concentration present in the Fe(III) enrichment medium (0.9g/L lactate/citrate) compared to *in-situ* DTMF conditions (10mg/L). It is however also possible that the isolated *Pseudomonas* spp. are specialized organisms, which have adapted to DTMF environments. *Rhodococcus* and *Clostridium* spp. are considered to be K-strategists, growing much slower while at the same time forming long term survival structures (De Leij *et al*, 1995, Juteau *et al*, 1999, Polyanskaya *et al*, 2002). K-strategists adapt to survival under crowded nutrient deficient conditions and are more resistant to various environmental stressors (Kozdroj *et al*, 1995). Therefore it is possible that the *Clostridium* and *Rhodococcus* spp. are more representative of the DTMF community.

Pseudomonas spp. have been documented to perform Fe(III) reduction while oxidizing a variety of electron donors (Lovley *et al.*, 1988, Hersman *et al.*, 2000) and have been isolated from heavy metal and uranium contaminated sites as shown in Table 3.1 as well as being previously characterized under extreme temperature conditions such as the

arctic terrestrial and marine environments of Svalbard, Norway (Kim *et al.*, 2010). *Pseudomonas* spp. are organisms part of the *Proteobacteria* group and closely related to *Shewanella* species, as well as being facultative anaerobic organisms (Hersman *et al.*, 2000, Lloyd 2003).

Table 3.1. DGGE band sequencing results.

Band number	Percentage	GenBank Closest match
1	99%	Uncultured <i>Pseudomonas</i> spp. clone FRC590 from uranium contaminated subsurface sediments (EU268627)
2	100%	<i>Pseudomonas</i> spp. KOPRI 25489 from arctic environment (GU062545)
3	100%	Uncultured <i>Clostridium</i> spp. clone FRC549 from uranium contaminated subsurface sediments (EU268613)
4	100%	<i>Rhodococcus</i> spp. PE2 KH4 from arsenic-rich neutral mine drainage tailings near Pezinok, Slovakia (HM047868)

It is thus possible that the isolated *Pseudomonas* spp. are well equipped for metabolic activity in subsurface environments as well as accustomed to environments relevant to *in-situ* conditions of the DTMF (oligotrophic, high heavy metal concentrations, high pH). *Clostridium* spp. which are strict anaerobic organisms, have also been documented to perform heavy metal reduction in uranium contaminated sediments and specifically Fe(III) reduction in freshwater sediment environments (Francis *et al.*, 1994, Francis 1998, Dobbin *et al.*, 1999, Holmes *et al.*, 2002). *Rhodococcus* species have been isolated from environments where metal oxides provide a suitable substrate for bioleaching processes and have been documented as As resisting bacteria (Krebs *et al.*, 1997, Zhao *et al.*, 2009). Based on the characteristics of these species and their suitability for the DTMF conditions, this microbial consortium is evidently capable of Fe(III) reduction in oligotrophic extreme pH and temperature environments (although low temperatures have not been tested in this study), whether as a symbiotic relationship of multiple species or individual metabolic pathways for energy conservation.

CHAPTER 4: CONCLUSIONS

4.1. Concluding Statement

The purpose of this study was to determine the rate of microbial Fe(III) reduction and formation potential of biofilm by the tailings-isolated mixed community under both bacterial growth favorable conditions and *in situ* conditions in terms of organic carbon content and pH. The hypothesis was that the redox potential in the DTMF sediment is influenced by microbial activity acting as a biological catalyst on the reduction of insoluble Fe(III) complexes such as ferrihydrite and ferric (hydr)oxide, causing the solubilization of associated heavy metals. The flow-cell systems used in this study facilitated the recording of measurable trends to determine microbial metabolic activity under both favorable and *in-situ* oligotrophic conditions. The mixed microbial community isolated from the DTMF sediment have shown the ability to reduce Fe(III) in an anaerobic environment under both high and low carbon conditions, neutral and high pH respectively. Although microbial metabolic rate was significantly decreased by carbon deprivation, an increase in incubation time of the flow-cell system might yield results which would describe a more significant pattern. It is unclear whether the community members are related through a symbiotic relationship from a metabolic perspective or whether each organisms acquired energy through a different pathway, but the microbial reduction of Fe(III) from a soluble source was achieved throughout the 8 day incubation period. Under high carbon conditions the mixed community was also capable of forming copious amounts of biofilm on the attachment substrate through formation of EPS, a network through which cells could adhere on the clay-sand surface, aggregate and possibly communicate. Under low carbon conditions, the microbial growth did not present with copious biofilm formation, but rather the cells decreased significantly in size and appeared as micro-colonies in areas of highest synthetic feed flow.

Although the isolated consortium was capable of Fe(III) reduction at a micro-scale, the overall impact on the DTMF sediment is still unknown. Due to the high pH buffering capacity of the tailings caused by high concentrations of lime, heavy metals solubilized in small microbial microcosms would probably quickly revert back to the immobilized form by

the bulk high pH outside the micro-environment. Nonetheless, under anaerobic environments such as sediments and tailings, microbial proliferation is based on using electron acceptors other than oxygen. Under environments where oxyanions and heavy metal complexes are abundant, such chemical species often provide the requirements for redox reactions performed for microbial energy conservation. The requirement of determining heavy metal stability up to 10,000 years in the DTMF certainly requires more study before an accurate prediction can be made. It is possible that microbial metabolic activity will remain insignificant to the bulk tailings body, but it may also be possible that highly reduced environments can develop at interfaces, given enough time.

4.2 Future Directions: Opportunities for Microbiological Studies

Future studies on the impact of microbiological activity will also focus on the interface area between the tailings sediment and the overlaying water. It is possible that this area of the tailings may experience higher metabolic activity due to potentially higher concentrations and sustained supply of available carbon. The metabolic activity and reducing power of mixed communities described in this study will be used as predictions for carbon depletion rates while future batch (enrichment) and column (flow-system) set-ups will be used to test such predictions and determine degree of carbon cycling that may be possible. The batch cultures will also be used as a means of differentiating between the dominant members in the *in situ* tailings material and the possible metal reducing specialized microorganisms that could be enriched from the tailings in the presence of final electron acceptors such as Fe(III), As(V) and SO_4^{2-} , using basic molecular techniques. This will clarify whether any metal reducing microbial species are metabolically active and abundant in the tailings material.

The flow-systems will be an excellent tool for quantifying microbial metabolic rates in the presence of the final electron acceptors mentioned above, through continuous monitoring of CO_2 production, pH, redox potential as well as analytical measurements of heavy metal concentrations downstream from the microbial activity site. These systems will be kept at various temperatures, which could help clarify the impact of microbial activity on

tailings geochemistry under *in situ* conditions. It is clear that such a study offers excellent opportunity for a better understanding and insight of microbial activity in highly selective environments such as the DTMF and how these processes apply to large scale systems.

REFERENCES

- Ahmann D., Krumholz L.R., Hemond H.F., Lovley D.R., Morel F.M.M.. 1997. Microbial mobilization of arsenic from sediments of the aberjona watershed. *Environmental Science and Technology* **31**(10): 2923-2930.
- Amann R.I., Stromley J., Devereux R., Key R., Stahl D.A.. 1992. Molecular and microscopic identification of sulfate-reducing bacteria in multispecies biofilms. *Applied and Environmental Microbiology* **58**(2): 614-623.
- Beliaev A.S., Saffarini D.A.. 1998. *Shewanella putrefaciens mtrB* encodes an outer membrane protein required for Fe(III) and Mn(IV) reduction. *Journal of Bacteriology* **180**(23): 6292-6297.
- Bristow C.M., Palmer Q., Witte G.J., Bowditch I., Howe J.H.. 2002. The ball clay and China clay industries of southwest England in 2000 – Industrial minerals and extractive industry geology. Scott P.W., Bristow C.M.. Geological Society of London, Alden Press, UK.
- Cameco Corporation. 2010. Mining: uranium operations; Saskatoon, Saskatchewan.
- Chao T.T.. 1972. Selective dissolution of manganese oxides from soils and sediments with acidified hydroxylamine hydrochloride. *Soil Science Society of America* **36**(5): 764-768.
- Coates J.D., Phillips E.J.P., Lonergan D.J., Jenter H., Lovley D.R.. 1996. Isolation of *Geobacter* species from diverse sedimentary environments. *Applied and Environmental Microbiology* **62**(5): 1531-1536.
- Coy Laboratory Products Inc. 2002. Model 10 gas analyzer instruction manual. Grass Lake, Michigan. 13-17.
- Cummings D.E., Caccavo F. Jr., Fendorf S., Rosenzweig F.R.. 1999. Arsenic mobilization by the dissimilatory Fe(III)-reducing bacterium *Shewanella alga* BrY. *Environmental Science and Technology* **33**(5): 723-729.
- De Leij F.A.A.M., Sutton E.J., Whipps J.M., Fenlon J.S., Lynch J.M.. 1995. Impact of field release of genetically modified *Pseudomonas fluorescens* on indigenous microbial populations of wheat. *Applied and Environmental Microbiology* **61**(9): 3443-3453.
- Delory G.E.. 1945. A sodium carbonate-bicarbonate buffer for alkaline phosphatases. *Biochemical Journal* **39**(3): 245.

DiChristina T.J., DeLong E.F.. 1994. Isolation of anaerobic respiratory mutants of *Shewanella putrefaciens* and genetic analysis of mutants deficient in anaerobic growth on Fe³⁺. *Journal of Bacteriology* **176**(5): 1468-1474.

Dobbin P.S., Carter J.P., San-Juan C.G.S., Hobe M., Powell A.K., Richardson D.J. 1999. Dissimilatory Fe(III) reduction by *Clostridium beijerinckii* isolated from freshwater sediment using Fe(III) maltol enrichment. *FEMS Microbiology Letters* **176**(1): 131-138.

Donahue R., Hendry M.J.. 2003. Geochemistry of arsenic in uranium mill tailings, Saskatchewan, Canada. *Applied Geochemistry* **18**(11): 1733-1750.

Elder, J.F. 1988. Metal biogeochemistry in surface-water systems - A review of principles and concepts. U.S. Geological Survey Circular 1013.

Francis A.J.. 1998. Biotransformation of uranium and other actinides in radioactive wastes. *Journal of Alloys and Compounds* **271-273**: 78-84.

Francis A.J., Dodge C.J., Lu F., Halads G.P., Clayton C.R.. 1994. XPS and XANES studies of uranium Reduction by *Clostridium* sp.. *Environmental Science and Technology* **28**(4): 636-639.

Fredrickson J.K., Romine M.F., Beliaev A.S., Auchtung J.M., Driscoll M.E., Gardner T S., Nealson K.H., Osterman A.L., Pinchuk G., Reed J.L., Rodionov D.A., Rodrigues J.L.M., Saffarini D.A., Serres M.H., Spormann A.M., Zhullin I.B., Tiedje J.M.. 2008. Towards environmental systems biology of *Shewanella*. *Nature Reviews* **6**: 592-603.

Gates W.P., Wilkinson H.T., Stucki J.W.. 1993. Swelling properties of microbially reduced ferruginous smectite. *Clay and Clay Minerals* **41**(3): 360-364.

Gerlach R., Cunningham A.B., Caccavo F. Jr.. 2000. Dissimilatory iron-reducing bacteria can influence the reduction of carbon tetrachloride by iron metal. *Environmental Science and Technology* **34**(12): 2461-2464.

Hall T.A.. 1999. BioEdit: a user-friendly biological sequence alignment editor and analysis program for windows 95/98/NT. *Nucleic Acids Symposium Series No.41*. Oxford University Press.

Hersman L.E., Forsythe J.H., Ticknor L.O., Maurice P.A.. 2001. Growth of *Pseudomonas mendocina*, on Fe(III) (hydr)oxides. *Applied and Environmental Microbiology* **67**(10): 4448-4453.

Hopper R.. 2000. Kinds of clay - Clay and glazes for the potter. Rhodes D. Krause Publications, US.

- Holmes D.E., Finneran K.T., O'Neil R.A., Lovley D.R.. 2002. Enrichment of members of the family *Geobacteraceae* associated with stimulation of dissimilatory metal reduction in uranium-contaminated aquifer sediments. *American Society for Microbiology* **68**(5): 2300-2306.
- Hudson-Edwards K.A., Schell C., Macklin M.G.. 1999. Minerology and geochemistry of alluvium contaminated by metal mining in the Rio Tinto area, southwest Spain. *Applied Geochemistry* **14**(8): 1015-1030.
- Islam F.S., Gault A.G., Boothman C., Poyla A.D., Charnock M.J., Chatterjee D., Lloyd J.R.. 2004. Role of metal-reducing bacteria in arsenic release from Bengal Delta sediments. *Nature* **430**: 68-71.
- Jackson M.L.. 2005. Redox potential measurement for soil – Soil chemical analysis: Second edition. Parallel Press, Wisconsin.
- Jacob H.E.. 1970. Redox potential – Methods in microbiology: Volume 2. Norris J.R., Ribbons D.W.. Academic Press, London.
- Jefferies M.G.. 1988. Determination of horizontal geostatic stress in clay with self-bored pressuremeter. *Canadian Geotechnical Journal* **25**(3): 559-573.
- Jones J.G., Davison W., Gardener S.. 1984. Iron reduction by bacteria: range of organisms involved and metals reduced. *FEMS Microbiology Letters* **21**(1): 133-136.
- Juteau P., Larocque R., Rho D., LeDuy A.. 1999. Analysis of the relative abundance of different types of bacteria capable of toluene degradation in a compost biofilter. *Applied Microbial Biotechnology* **52**(6): 863-868.
- Kiernan J.A.. 2000. Formaldehyde, formalin, paraformaldehyde and glutaraldehyde: What they are and what they do. *Microscopy Today* **00-1**: 8-12.
- Kim E.H, Cho H.K., Lee Y.M., Yim J.H., Lee H.K., Cho J.C., Hong S.G.. 2010. Diversity of cold-active protease-producing bacteria from arctic terrestrial and marine environments by enrichment culture. *The Journal of Microbiology* **48**(4): 426-432.
- Kostka J.E., Stucki J.W., Nealson K.H., Wu J.. 1996. Reduction of structural Fe(III) in smectite by a pure culture of *Shewanella putrefaciens* strain MR-1. *Clays and Clay Minerals* **44**(4): 522-529.
- Kostka J.E., Dalton D.D., Skelton H., Dollhopf S., Stucki W.J.. 2002. Growth of iron(III)-reducing bacteria on clay minerals as the sole electron acceptor and comparison of growth yields on a variety of oxidized iron forms. *Applied and Environmental Microbiology* **68**(12): 6256-6262.

Kozdroj J., Piotrowska-Seget Z.. 1995. Indigenous microflora and bean responses to introduction of genetically modified *Pseudomonas fluorescens* strains into soil contaminated with copper. *Journal of Environmental Science and Health*. **30**(10): 2133-2158.

Lee J.U., Lee S.W., Chon H.T., Kim K.W., Lee J.S.. 2008. Enhancement of arsenic mobility by indigenous bacteria from mine tailings as response to organic supply. *Environment International* **35**(3): 496-501.

Lee S., Malone C., Kemp P.F.. 1993. Use of multiple 16S rRNA-targeted fluorescent probes to increase signal strength and measure cellular RNA from natural planktonic bacteria. *Marine Ecology Progress Series* **101**: 193-201

Lim M.S., Yeo I.W., Roh Y., Lee K.K., Jung M.C.. 2008. Arsenic reduction and precipitation by *Shewanella* sp.: batch and column tests. *Geosciences Journal* **12**(2): 151-157.

Lloyd J.R.. 2003. Microbial reduction of metals and radionuclides. *FEMS Microbiology Reviews* **27**(2-3): 411-425.

Lonergan D.J., Jenter H.I., Coates J.D., Phillips E.J.P., Schmidt T.M., Lovley D.R.. 1996. Phylogenetic analysis of dissimilatory Fe(III)-reducing bacteria. *Journal of Bacteriology* **178**(8): 2402-2408.

Maathuis H.. 2010. Deilmann tailings management facility – 2009 tailings investigation and monitor well construction. Key Lake Operation, Geo-Environmental Engineering, Technical Services, Mining Division.

Masscheleyn P.H., Delaune R.D., Patrick W.H. Jr.. 1991. Arsenic and selenium chemistry as affected by sediment redox potential and pH. *Journal of Environmental Quality* **20**: 522-527.

Masscheleyn P.H., Delaune R.D., Patrick W.H. Jr.. 1991. Effect of redox potential and pH on arsenic speciation and solubility in a contaminated soil. *Environmental Science and Technology* **25**(8): 1414-1419.

Mladenov N., Zheng Y., Miller M.P., Nemergut D.R., Legg T., Simone B., Hageman C., Rahman M.M., Ahmed K.M., McKnight D.M.. 2010. Dissolved organic matter sources and consequences for iron and arsenic mobilization in Bangladesh aquifers. *Environmental Science and Technology* **44**(1): 123-128.

Moldovan J.B., Hendry J.M., Harrington G. A.. 2008. The arsenic source term for an in-pit uranium mine tailings facility and its long-term impact on the regional groundwater. *Applied Geochemistry* **23**(6): 1437-1450.

Natural Resources Canada. 2009. Energy sector – Uranium/nuclear energy: Uranium mine and mill tailings.

Natural Resources Canada. 2009. Energy sector – Uranium/nuclear energy: Tailings management.

Niggemeyer A., Spring S., Stackerbrandt E., Rosenzweig F.. 2001. Isolation and characterization of a novel As(V)-reducing bacterium: implications for arsenic mobilization and the genus *Desulfitobacterium*. Applied and Environmental Microbiology **67**(12): 5568-5580.

Obuekwe C.O., Westlake W.S.. 1982. Effects of medium composition on cell pigmentation, cytochrome content, and ferric iron reduction in a *Pseudomonad* sp. isolated from crude oil. Canadian Journal of Microbiology **28**(8): 989-992.

Oremland R.S., Saltikov C.W., Wolfe-Simon F., Stolz F.J.. 2009. Arsenic in the evolution of earth and extraterrestrial ecosystems. Geomicrobiology Journal **26**(7): 522-536.

Panak P., Hard B.C., Pietzsch K., Kutschke S., Roske K., Selenska-Pobell S., Bernhard G., Nitsche H.. 1998. Bacteria from uranium mining waste pile: interactions with U(VI). Journal of Alloys and Compounds **271-273**: 262-266.

Polyanskaya L.M., Vedina O.T., Lysak L.V., Zviagintsev D.G.. 2002. The growth promoting effect of *Beijerinckia* and *Clostridium* sp. cultures on some agricultural crops. Mikrobiologiya **71**(1): 123-129.

Postma D., Jakobsen R.. 1996. Redox zonation: equilibrium constraints on the Fe(III)/SO₄-reduction interface. Geochimica et Cosmochimica Acta **60**(17): 3169-3175.

Rah Y., Chon C.M., Moon J.W.. 2007. Metal reduction and biomineralization by an alkaliphilic metal-reducing Bacterium, *Alkaliphilus metalliredigens* (QYMF). Geosciences Journal **11**(4): 415-423.

Ribet I., Ptacek C.J., Blowes D.W., Jambor J.L.. 1995. The potential for metal release by reductive dissolution of weathered mine tailings. Journal of Contaminant Hydrology **17**(3): 239-273.

Rump H.H.. 1999. Field measurements – laboratory manual for the examination of water, waste water and soil: Third Edition. Wiley-VCH Verlag, Germany.

Saltikov C.W., Wildman R A. Jr., Newman D.K.. 2005. Expression dynamics of arsenic respiration and detoxification in *Shewanella* sp. strain ANA-3. Journal of Bacteriology **187**(21): 7390-7396.

Stookey, L.L.. 1970. Ferrozine: a new spectrophotometric reagent for iron. Analytical Chemistry **42**(7): 779-781.

Straub K.L., Benz M., Schink B.. 2001. Iron metabolism in anoxic environments at near neutral pH. *FEMS Microbiology Ecology* **34**(3): 181-186.

Siddique T., Arocena J.M., Thring R.W., Zhang Y.. 2007. Bacterial reduction of selenium in coal mine tailings pond sediment. *Journal of Environmental Quality* **36**(3): 621-627.

Tessier A., Fortin D., Belzile N., DeVitre R.R., Lepard G.G.. 1996. Metal sorption to diagenetic iron and manganese oxyhydroxides and associated organic matter: narrowing the gap between field and laboratory measurements. *Geochimica et Cosmochimica Acta* **60**(3): 387-404.

Thamdrup B.. 2000. Bacterial manganese and iron reduction in aquatic sediments – advances in microbial ecology: Volume 16. Schink B.. Kluwer Academic/Plenum Publishers, New York.

U.S. Energy Information Administration. 2010. International energy outlook. U.S. Department of Energy, Washington, DC.

Viollier E., Inglett P.W., Hunter K., Roychoudhury A.N., Cappellen P.V.. 2000. The ferrozine method revisited: Fe(II)/Fe(III) determination in natural waters. *Applied Geochemistry* **15**(6): 785-790.

Wimpenny J.W.T., Necklen D.K.. 1971. The redox environment and microbial physiology. *Biochemica Et Biophysica Acta* **253**(2): 352-359.

Wolfaardt G.M., Hendry M.J., Korber D.R.. 2008. Microbial distribution and diversity in saturated high pH, uranium mine tailings, Saskatchewan, Canada. *Canadian Journal of Microbiology* **54**(11): 932-940.

World Nuclear Association. 2010. World Energy Needs and Nuclear Power. London, UK.

Yatsenko N.D., Verevkin K.A., Zubekhin A.P.. 2010. Mössbauer spectroscopy of phase and crystal-chemical states of iron oxides in ceramic brick. *Glass and Ceramics* **67**(5-6): 176-178.

APPENDICES

Appendix 1: Physical and Chemical Measurements of DTMF Core Samples

Table A1.1 Physical and chemical measurements of the DTMF cores at the E2 site.

Core Number	Depth (m)	Average pH	Average Eh (mV)	Pore Waters Dissolved Organic Carbon (mg/L)	Tailings Organic Carbon (%/g)	Fe(III) Tailings Concentrations (mg/g)
C-1	50.65 - 53.65	10.6	275.67	12	0.76	12
C-2	53.65 - 56.65	10.7	202.33	2.5	0.62	8.7
C-3	56.65 - 59.65	10.5	238.33	6.2	0.57	5.9
C-4	59.65 - 62.65	9.7	276.00	7.7	0.12	3.4
C- SAND	62.65 - 64.65	7.9	344.33	7.2	0.06	1.4
C-SAND	64.65 - 67.65	7.4	351.00	9.9	0.32	8.1
C-SAND	67.65 - 70.65	7.4	285.00	20	0.76	5.3
C-5	71.65 - 74.65	10.0	99.50	9.8	0.57	9.8
C-6	74.65 - 77.65	10.0	204.80	6.6	0.84	16.7
C-7	77.65 - 80.65	10.0	175.80	7.2	0.97	16.8
C-8	80.65 - 83.65	9.9	67.30	12	0.91	13.5
C-9	83.65 - 86.65	10.2	141.20	7.2	1.48	8.2
C-10	89.65 - 92.65	9.7	146.50	8.8	0.91	10.3
C-11	92.65 - 95.65	10.1	162.80	16	0.73	10
C-12	95.65 - 98.65	9.8	124.30	18	0.74	15.6
C-13	98.65 - 101.65	10.0	68.00	16	0.98	17.7
C-14	101.65 - 104.65	10.1	103.00	8.8	0.98	18.7
C-15	104.65 - 107.65	11.2	-178.00	8.6	0.86	20.6
C-16	107.65 - 110.65	9.8	-233.30	16	0.53	19.7
C-17	110.65 - 113.65	10.3	-243.70	18	0.46	16.4
C-18	113.65 - 116.65	10.1	118.50	16	0.56	15.6
C-19	116.65 - 119.65	11.2	-252.80	8.8	0.74	16.3
C-20	119.65 - 122.65	10.2	-261.00	8.6	0.87	16.2

- * Temperature readings could not be included due to values being offset by frictional forces of the drill head;
- * C-SAND indicates areas of tailings sloughing with sand from the Deilmann pit banks;
- * Sample #60 was taken from core #20; 3 biological samples were taken per core;

Appendix 2: Redox Potential Measurements: Continuous recorded OR values.

Table A2.1 Raw OR data sample recorded with the Symphony® SP70P portable pH/OR meter, in a mixed community flow-cell under low-carbon conditions at pH 9.5.

P70P PORTABLE PH METER	
Meter S/n	C02089
SW rev	2.60
Method #	10
10-12-2010 15:03:44	
mV	77.3 mV
Temperature	25.0 C
Log #	1
Operator	_____
Sample #	_____
P70P PORTABLE PH METER	
Meter S/n	C02089
SW rev	2.60
Method #	10
10-12-2010 16:03:52	
mV	-47.0 mV
Temperature	25.0 C
Log #	2
Operator	_____
Sample #	_____
P70P PORTABLE PH METER	
Meter S/n	C02089
SW rev	2.60
Method #	10
10-12-2010 17:03:52	
mV	-42.9 mV
Temperature	25.0 C
Log #	3
Operator	_____
Sample #	_____

Table A2.2 Redox Potential Measurements of flow-cells under high carbon conditions at pH 7.0.

Time (days)	Mixed Community	Positive Control	Sterile Control
	Redox Potential (mV)		
0	25	-20.2	-6.90
1	-148.2	-329.8	10.70
2	-148.2	-257.7	-5.60
3	-172.7	-267.2	-51.30
4	-184.7	-304.2	-76.40
5	-191.4	-368.7	-34.40
6	-203.4	-382.5	-22.90
7	-207.8	-366.4	32.70
8	-234.9	-348.6	41.00

Table A2.3 Redox Potential Measurements of flow-cells under low carbon conditions at pH 9.5.

Time (days)	Mixed Community	Positive Control	Sterile Control
	Redox Potential (mV)		
0	139.6	77.3	-6.90
1	31.7	-60.2	10.70
2	-15.8	-136.2	-5.60
3	-42.9	-170	-51.30
4	-69.9	-208.3	-76.40
5	-86.1	-259.1	-34.40
6	-100.8	-266	-22.90
7	-127.4	-279.2	32.70
8	-160.1	-305.7	41.00

Appendix 3: Ferrous Iron Concentration Measurements - The Ferrozine Method.

Table A3.1 Fe(II) standards for Mixed Community flow-cell, high carbon, neutral pH.

Standard Number	Fe ²⁺ Concentration (mg/L)	Absorbance			Mean Absorbance
1	2.5	0.0996	0.1009	0.1012	0.1006
2	5	0.1735	0.1794	0.1748	0.1759
3	7.5	0.298	0.2982	0.3081	0.3014
4	10	0.3914	0.394	0.3951	0.3935
5	12.5	0.5488	0.551	0.5494	0.5497
6	15	0.616	0.6209	0.6171	0.6180
7	17.5	0.731	0.7678	0.7792	0.7593
8	20	0.814	0.8228	0.8371	0.8246
9	23	0.9889	0.9968	0.9989	0.9949

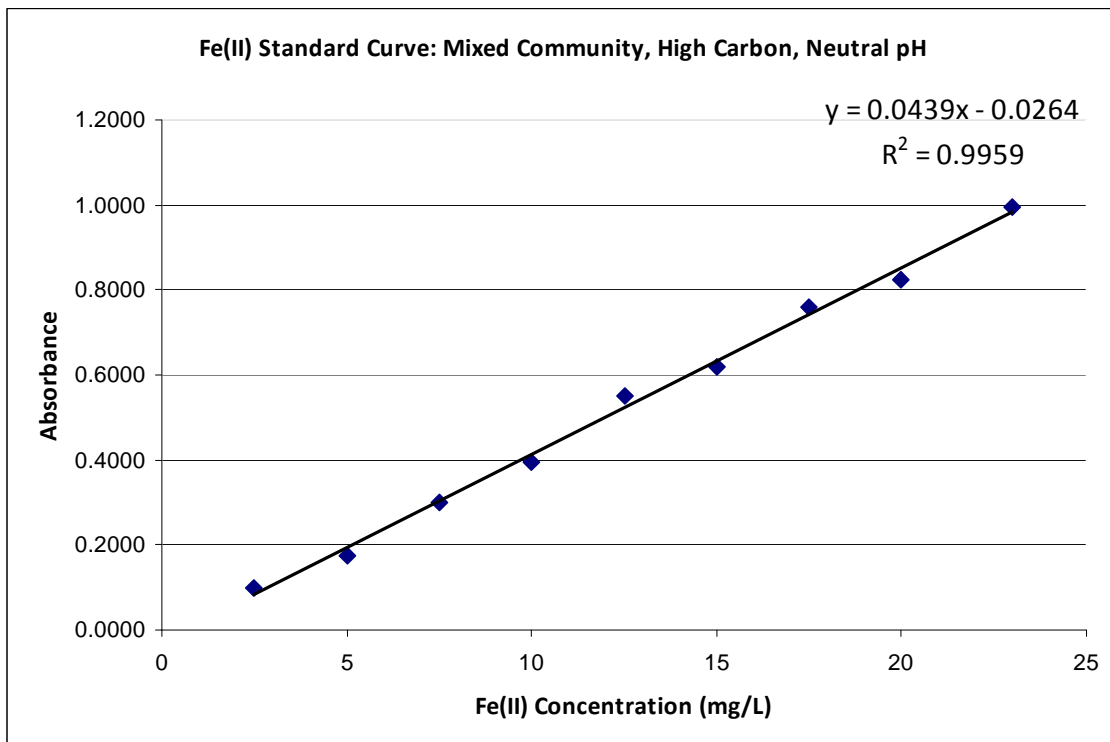


Figure A3.1. Fe(II) Standard Curve, Mixed community samples, high carbon, neutral pH.

Table A3.2 Mixed Community flow-cell samples ferrozine absorbance values.

Time (days)	Mixed Community Flow-cell Samples Absorbance		
0	0.2553	0.2312	0.2806
1	0.5752	0.5605	0.5706
2	0.3683	0.3491	0.3717
3	0.2475	0.2448	0.256
4	0.3633	0.3535	0.3874
5	0.4797	0.467	0.4926
6	0.6183	0.5996	0.6438
7	0.7387	0.7266	0.7349
8	0.6194	0.6289	0.5884

5X Dilution

Table A3.3 Mixed Community Fe(II) concentrations in high carbon neutral pH flow-cell.

Time (days)	Mixed Community Flow-cell Fe(II) Concentrations (mg/L)			Mean Fe(II) Concentration (mg/L)	Standard Deviation
0	6.417	5.87	6.99	6.43	0.56
1	13.704	13.37	13.60	13.56	0.17
2	44.954	42.77	45.34	44.35	1.39
3	31.196	30.89	32.16	31.42	0.67
4	44.385	43.27	47.13	44.93	1.99
5	57.642	56.20	59.11	57.65	1.46
6	73.428	71.30	76.33	73.69	2.53
7	87.141	85.76	86.71	86.54	0.70
8	73.554	74.64	70.02	72.74	2.41

Table A3.4 Positive Control Fe(II) concentrations in high carbon neutral pH flow-cell.

Time (Days)	Positive Control Fow-cell Fe(II) Concentrations (mg/L)			Mean Fe(II) Concentrations (mg/L)	Standard Deviation
0	9.00	8.94	8.79	8.91	0.11
1	198.48	193.49	194.40	195.46	2.66
2	193.86	193.33	195.20	194.13	0.97
3	201.43	202.83	204.14	202.80	1.36
4	199.29	201.16	203.07	201.17	1.89
5	201.56	197.88	201.26	200.23	2.04
6	199.19	201.93	200.06	200.39	1.40
7	190.04	191.85	192.92	191.61	1.46
8	153.95	180.17	181.41	171.84	15.51

Table A3.5 Sterile Control Fe(II) concentrations in high carbon neutral pH flow-cell.

Time (days)	Sterile Control Flow-cell Fe(II) Concentrations (mg/L)			Mean Fe(II) Concentrations (mg/L)	Standard Deviation
0	7.36	7.03	7.26	7.21	0.17
1	7.21	6.79	7.29	7.10	0.27
2	8.46	7.95	8.64	8.35	0.36
3	6.54	6.32	7.08	6.65	0.39
4	7.49	7.20	7.77	7.49	0.28
5	7.95	7.54	8.52	8.00	0.49
6	14.43	14.16	14.35	14.31	0.14
7	17.73	17.94	17.04	17.57	0.47
8	17.98	17.45	18.54	17.99	0.55

Table A3.6 Mixed Community Fe(II) concentrations in low carbon flow-cell, pH 9.5.

Time (Days)	Mixed Community Flow-cell Fe(II) Concentrations (mg/L)			Mean Fe(II) Concentrations (mg/L)	Standard Deviation
0	2.94	4.12	4.01	3.69	0.65
1	2.83	3.17	3.10	3.03	0.18
2	6.18	7.40	6.65	6.74	0.61
3	6.72	7.49	7.55	7.25	0.46
4	9.46	10.14	10.30	9.97	0.44
5	9.20	10.31	9.77	9.76	0.56
6	12.57	12.62	12.67	12.62	0.05
7	12.16	13.02	12.94	12.71	0.47
8	14.09	14.98	14.79	14.62	0.47

Table A3.7 Positive Control Fe(II) concentrations in low carbon flow-cell, pH 9.5.

Time (days)	Positive Control Flow-cell Fe(II) Concentrations (mg/L)			Mean Fe(II) Concentrations (mg/L)	Standard Deviation
0	4.19	3.06	3.52	3.59	0.57
1	23.05	23.50	23.63	23.40	0.30
2	35.96	37.40	36.78	36.71	0.72
3	44.46	44.37	43.75	44.19	0.39
4	43.40	42.95	42.95	43.10	0.26
5	44.16	44.93	45.03	44.71	0.48
6	43.27	42.71	48.77	44.92	3.35
7	46.27	46.95	45.69	46.30	0.63
8	49.57	51.91	50.35	50.61	1.19

*** The same sterile control data was used for both high carbon and low carbon experiments.**